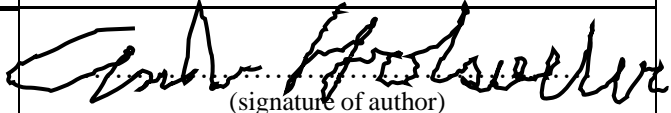




Universitetet
i Stavanger

FACULTY OF SCIENCE AND TECHNOLOGY

MASTER'S THESIS

Study program/specialization: Petroleum Engineering (Well Engineering)	Spring 2017 Open
Author: Andrew Martin Holsaeter	 (signature of author)
Programme coordinator: Dan Sui Supervisor(s): Dan Sui	
Title of master's thesis: Integration of modeling and drilling incident management of a real-time lab-scale autonomous drilling rig	
Study points: 30	
Keywords: Automation Drill-string Modeling Data Acquisition and Handling Real-time System Design Drilling Optimization	Number of pages: 45 + supplemental material/other: 52 Stavanger, 29 June 2017

Acknowledgements

First and foremost, I would like to thank Dan Sui for her constant support and guidance.

I would also like to thank my external project supervisor, Robert Ewald, for his patience and help guiding me through coding and programing an entire autonomous system with zero experience beforehand.

Also, I would like to give a special thank you to our team leader, Erik Løken, for always believing in me and constantly pushing me.

Lastly, I would like to thank my parents for their constant love and support to push me to pursue my dreams.

Abstract

The basis of this thesis is an attempt to design, construct, and implement a fully autonomous lab scale drilling rig with real time optimization and capable of drilling detection and subsequent mitigation. Two simplified drill-string models are applied to be used in ROP models for drilling optimization. Several drilling problems pertinent to a small-scale rig are discussed with solutions to identify and mitigation procedures are proposed. This thesis also goes in to the necessity control system and data acquisition tools, such as filtering, system coordination, human machine interface (HMI), etc.... required to create a real-time lab scale autonomous rig.

Chapter 1 - Introduction

With increased cost of drilling and low oil prices, autonomous drilling has become of more and more interest to the drilling community. However, despite the appeal of replacing humans with smart machines, there are several problems with autonomous drilling such as the slower speed and a lack of field testing

With this in mind, a lab-scale drilling rig, approximately two meters in height, was constructed from scratch with a budget of approximately \$20,000 USD. The purpose of the rig was to compete in the annual autonomous drilling competition hosted by the Drilling Systems Automation Technical Section (DSATS) of SPE as well as further research and training of drilling principles to university students.

Paramount to the success of this rig was the proper data acquisition and handling as well as the programming necessary to make such a rig successful. As the lead software engineer with no background before coming onto this project six months ago, this paper delves into how it is possible to implement such a system with such limited experience.

This paper discusses several models that can be applied to an autonomous rig, the requirements to build such a rig, and some examples of associated drilling problems and possible mitigations. It also offers some proposals to better improve drilling rigs in the future.

Chapter 2 - Rig Design

The drilling has three main systems: circulation, hoisting, and top drive. Each system has their own programmable logic controller (PLC) which communicate to each other through a coordinator class in the computer strategic controller. This is discussed in more detail in chapter 4.

Circulation

The main purpose of a circulation system is to remove cuttings from the wellbore and lubricate and cool down the downhole assembly. On such a small scale, however, the temperature effects are negligible as are most of the lubricating effects. Below is a basic outline of the circulation system.

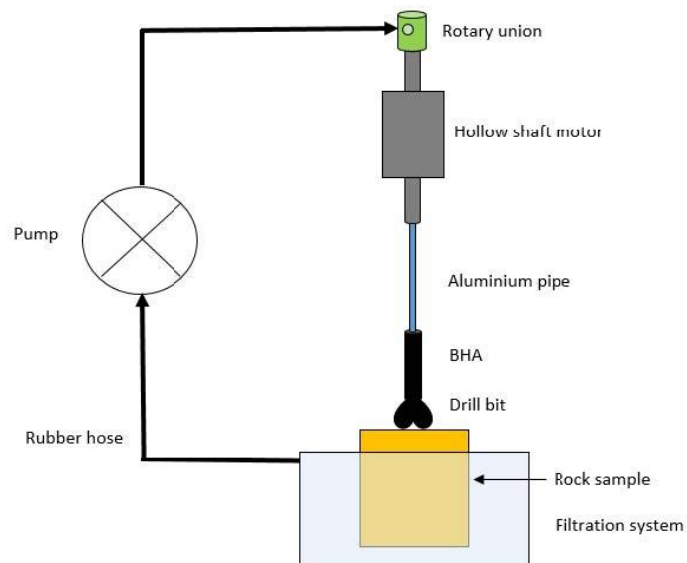


Fig. 2.1: Circulation outline diagram

Once the pump was installed, a pump characteristics curve was created for the pump.

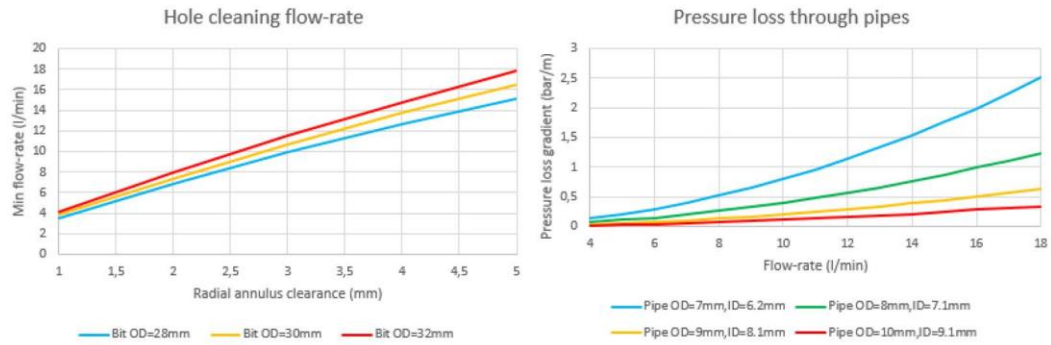


Fig. 2.2: Flow rates and pressure losses for different diameters

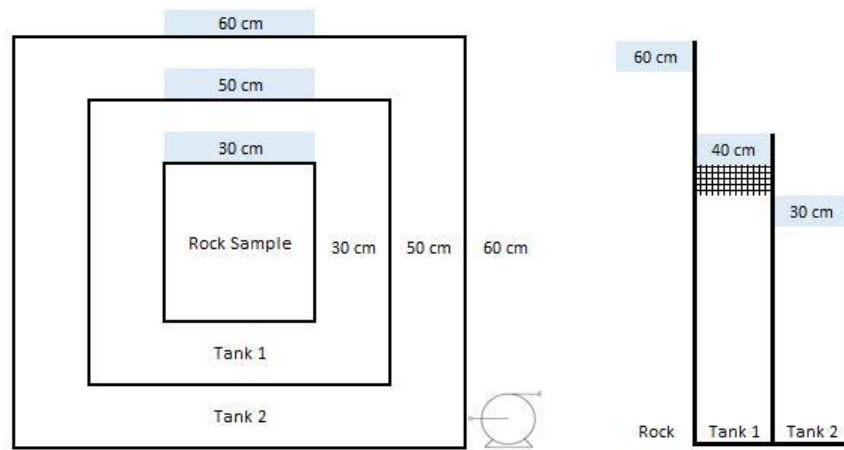


Fig. 2.3: Deposit tank system schematics

Below are the design calculations.

- Hole Volume = $3.847 \times 10^{-4} \text{ m}^3 = 384 \text{ cm}^3$
- Maximum flow rate = 18.5 liters per minute = $18500 \text{ cm}^3/\text{min}$
- Initial volume in inner tank = 0
- Initial volume in outer tank = 33 L
- Area of rock = 900 cm^2

Minimum required mesh areas and box lengths for the entire duration of drilling:

- Tank 1: Effective area (m^2) – 0.16, Volume (L) – 64
- Tank 2: Effective area (m^2) – 0.11, Volume (L) – 33

This results in the following times:

- Pump to bit = 0.09 minutes
- Bit to rock surface = 0.02 minutes
- Full tank 1 to overflow into tank 2 = 3.46 minutes
- Total flow loop time = 3.57 minutes = 3 minutes 34 seconds

Hoisting

Hoisting is comprised of a top plate attached to three independent actuators via their own triaxial bi-directional load cells with a range of -100N to 100N. The actuators had a lead screw with a pitch of 8mm, each with a triaxial load cell. They are driven by Nema 23 stepper motors with 2000 microsteps per rotation through individual drivers from a common hoisting programmable logic controller (PLC). Thus, the resolution of the actuator control is 0.004 mm. As shown in figure 5.4, this corresponds approximately to a resolution of 0.06 kg or 60 g when drilling through concrete.

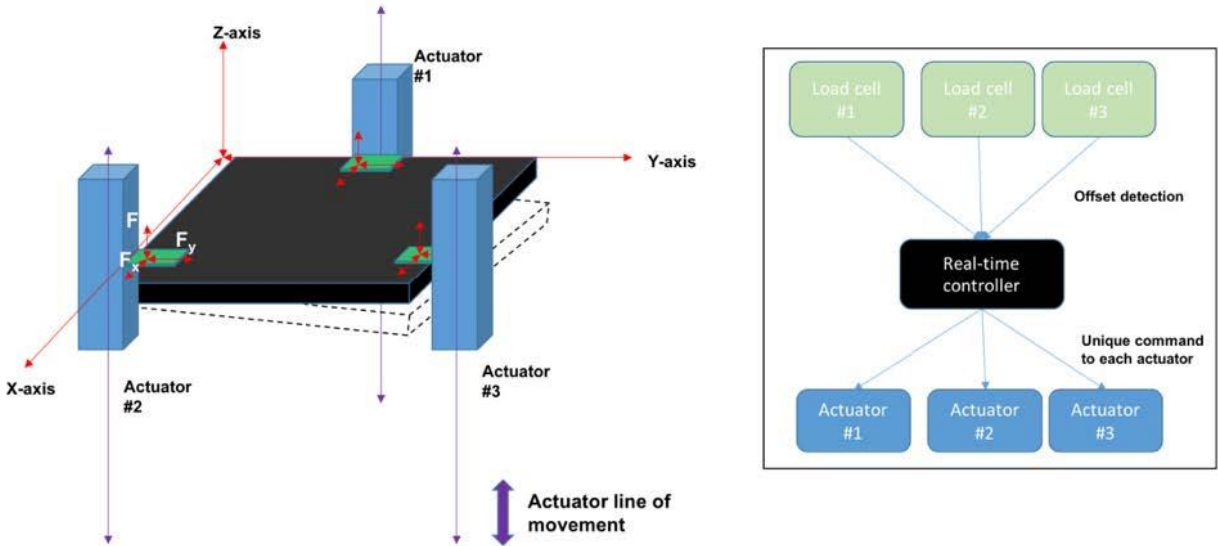


Fig 2.4: Hoisting design

Top Drive

The top drive is powered using a 900-watt brushless hollow-shaft motor with torque and rpm feedback being output through an encoder into its own top drive PLC. The purchased driver for the motor lets us define a torque motor limitation to cut off rotation which is set to the calculated value in chapter 5.

The maximum RPM was limited to approximately 900 RPM due to the operating capacity of the rotary union, but is also a function of the loop times due to twist off avoidance which is discussed more in detail in chapter 4.

Chapter 2 – Drilling Problems

The scope of this paper focuses primarily on a lab scale drilling rig. As such, only those drilling problems pertaining to a small-scale rig are discussed. For instance, temperature effects one of the most pertinent drilling problems in a full scale operation, but on such a small scale the temperature differences are extremely negligible.

Vibrations

Vibrations are one of the most common drilling problems and can be very complex. There are three types of vibrations that a drill-string experiences:

- 1) Axial
- 2) Lateral
- 3) Torsional

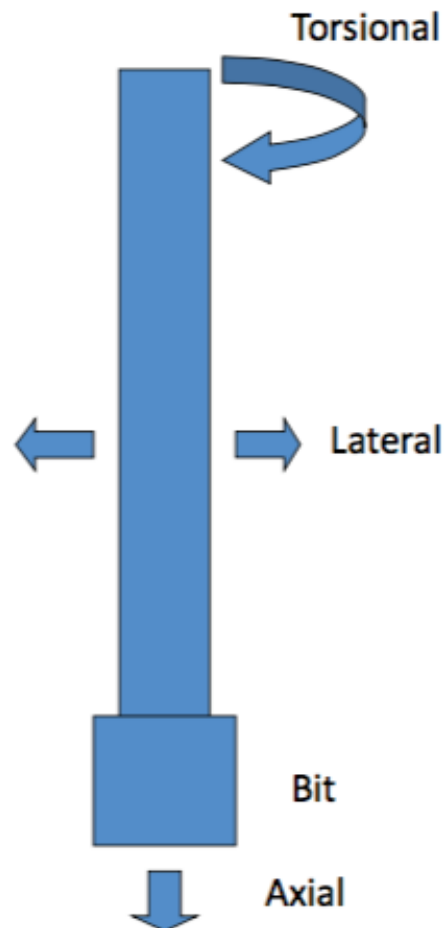


Fig. 2.5 Types of vibration drill-string experiences [1]

Axial Vibrations

This phenomenon occurs when the bit bounces up and down creating shockwaves along the drill-string. This type of drilling is more common when drilling with roller cone bits, but it can still be seen when drilling with PDC bits.

Whirl

There are three types of whirl that occur

- 1) Forward Whirl
- 2) Backward Whirl
- 3) Chaotic Whirl

Forward whirl is when the rotation is the same direction of the drill-string.

Backward whirl is when the rotation is in the opposite direction of the drill-string. This is caused by higher friction which increases the torque in the BHA and forces rotation in the opposite direction [1].

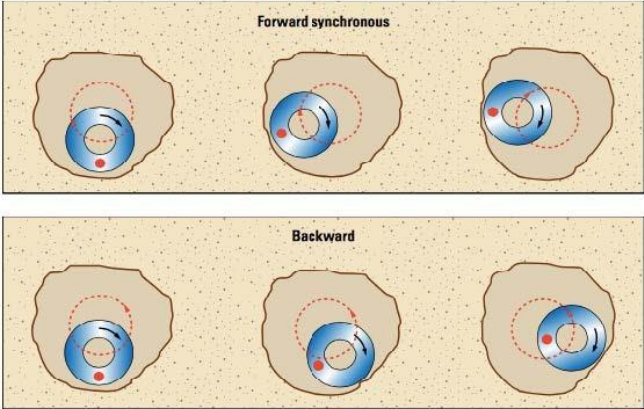


Fig. 2.6 Forward and backward whirl [1]

Stick-Slip

Stick-slip occurs when the drill-bit or any part of the BHA, gets “caught” bottom hole. The rotational speed falls to zero even though the top drive rotational speed remains constant. This increases the torque until either the “caught” part of the BHA overcomes the friction of the stuck part and releases or the torsional limit of the BHA is exceed causing catastrophic failure of the material.

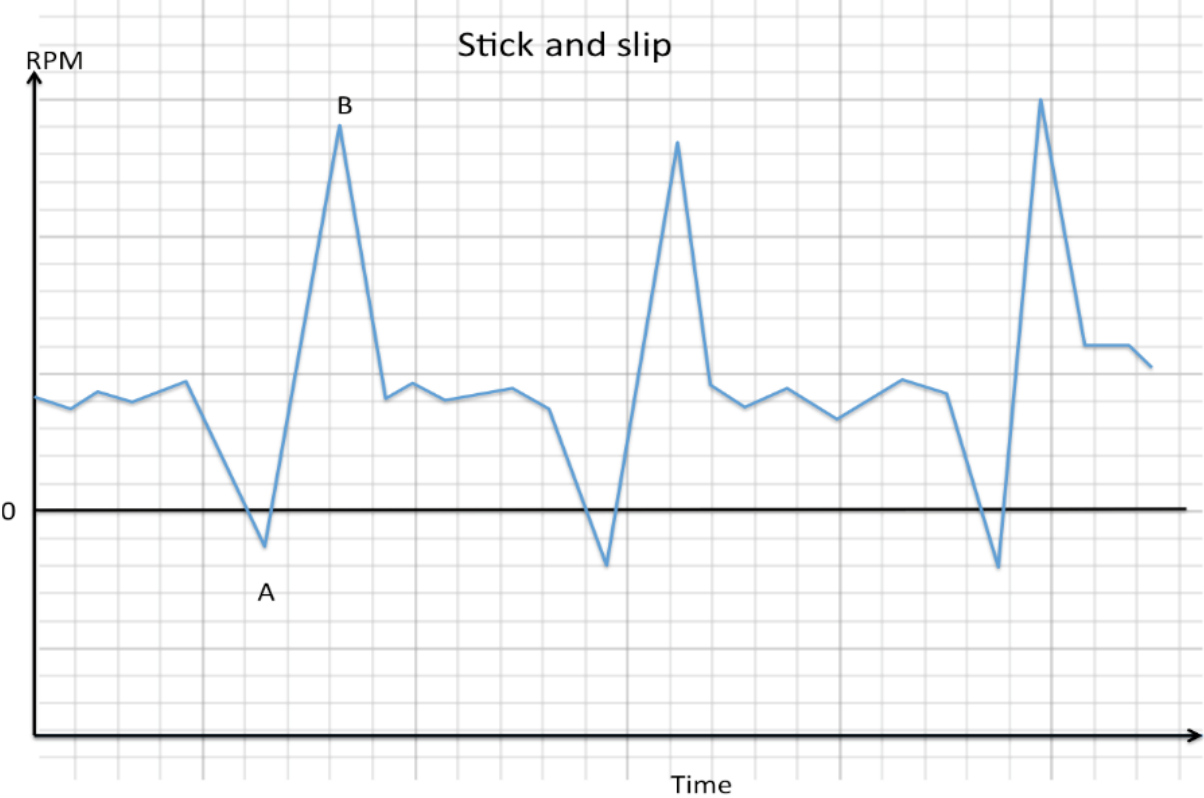


Fig. 2.7 Stick Slip [1]

Twist Off

Unlike in stick slip, if the torsional force increase is not released, it can exceed ultimate limit of material at which point a catastrophic failure occurs.

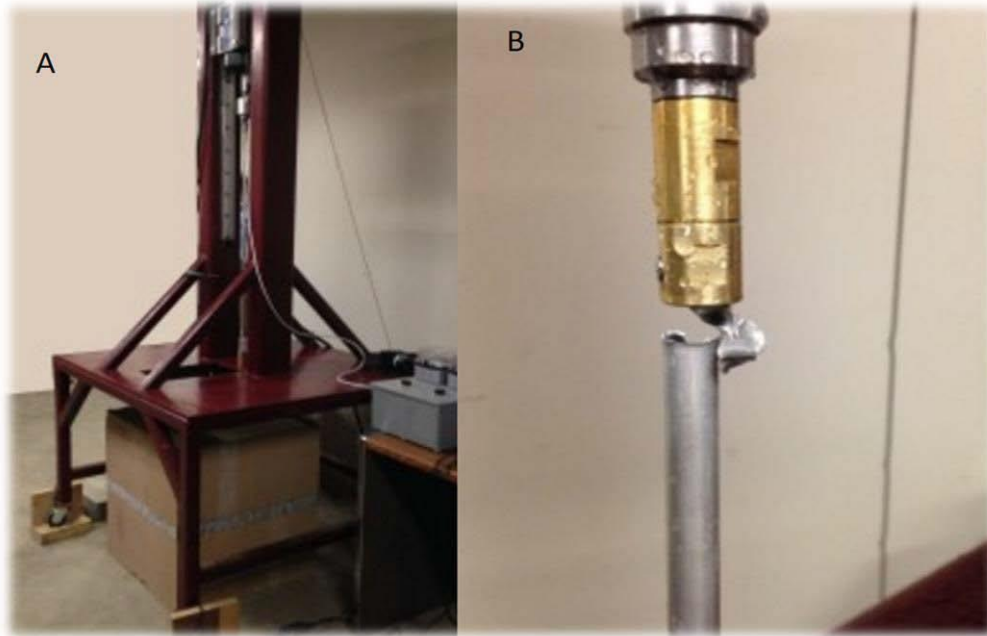


Fig. 2.8 *Twist off from Texas A&M rig in 2015 [2]*

Overpull

When tripping out of the wellbore, the drill string gets stuck and the tensile limit of any component of the drill string can exceed its critical tensile limit.

Pack-off

Flow somewhere along the drill string becomes clogged. This is usually caused by cuttings falling back in to the hole. This has a deteriorating effect on ROP and can cause other drilling problems such as overpull when trying to trip out.

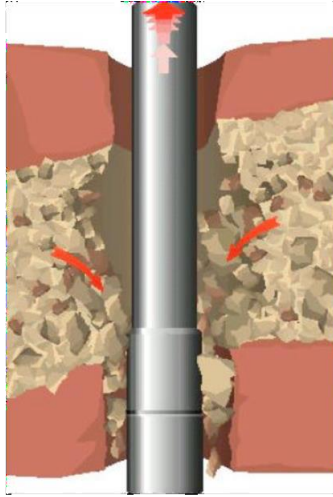


Fig. 2.9 *Pack off scenario [1]*

Washout

While a washout is highly unlikely in such as small rock sample with virtually no confined pressure, there is a similar scenario such as a leak.

Fault Detection

In order to detect individual problems, there must be a unique set of identifiers for each individual problem. This is limited the sensors we are using:

- * Forces in the z – direction
- * Forces in the x-y plane
- * Pressure at the pump
- * Motor torque
- * Stepper positions
- *Height sensor

Explicit Indications of Drilling Problems

It is important to have an explicit solution for each drilling scenario to ensure no ambiguity of drilling problem identification so as to ensure the correct remedial actions are executed. Below is a summary of each drilling problem, and the associated sensor values.

Stick-Slip

ROP - Decrease

Torque - Spikes

SPP - Unchanged

RPM - Spikes

WOB – Unchanged

Pack-off

ROP - Falls to zero

Torque - Gradual increase

SPP - Significant increase

RPM - Falls to zero

WOB - Falls to zero

Key Seating

ROP - Decrease

Torque - Increase slightly

SPP - Increase slightly

RPM - Unchanged

WOB - Decrease

Bit Balling/Clay Swelling

ROP - Tends to zero

Torque - Sharp decrease

SPP - Sharp increase

RPM - No change

WOB - Decrease to zero

Overpull

This will only occur when raising the bit and will be detected by the load cells in z direction sharply increasing

New Formation

In addition to these seven problems, we must also be able to identify a “new formation” in order to optimize ROP. Two proposed ways of doing this are by using MSE and/or d-exponent calculations

Remedial Actions

Axial Vibrations

Forces in the z-direction show erratic fluctuations. For our purposes, we divided axial vibrations into two scenarios

- 1) Normal Vibrations
- 2) Damaging Vibrations

It is important to mitigate normal vibrations in order to reduce problems, as they can be detrimental over long periods of time, and also to increase overall efficiency. Omdal Kjetil proposes tools on the market that can be used to help mitigate these problems, but that is outside the scope of this paper [3].

Normal vibrations are normal vibrations that one would expect during drilling. While no remedial action is needed immediately, long term normal vibrations can cause wear on the BHA and drill-bit. Normal vibrations are defined as fluctuations of ± 2.5 kg of the setpoint, i.e. an amplitude of 5 kg experienced in a short period of time. Every 50 samples were put into an array and if between 10 and 40 of these samples are on either side of these limits, normal vibrations are detected. The upper limit is introduced so that an overshoot of the PID controller does not falsely identify as vibrations. Although testing of the string showed that the drill-string could safely handle drilling in these conditions, ROP could be adversely affected.

Damaging vibrations, however, must be dealt with immediately as these could cause immediate damage to the drill-string and/or drill-bit. When damaging vibrations are encountered, the WOB is set to $0.9 \times$ the old WOB and RPM is set to the old RPM +50, and the new hard limits for the formation are set to these current WOB and RPM values.

Damaging vibrations are defined as fluctuations of ± 10 kg of the setpoint, i.e. an amplitude of 20 kg experienced in a short period of time. The same 50 sample data array for normal vibration detection are also evaluated to see if between 10 and 40 of these samples are on either side of these limits, immediate remedial actions are executed.

Lateral Vibrations

As with axial vibrations, lateral vibrations will show as large oscillations in the x and y directions.

Due to the design of this rig, lateral vibration mitigation is outside the scope of this paper as it requires separate tools to mitigate.

Overpull

The hoisting PLC is constantly checking for an overpull situation, as it won't be able to move a step if the any of the load cells exceed the overpull threshold (See Appendix C). If the threshold is exceeded, the coordinator will be notified and a command will be sent to overwrite the current command to send the hoisting down 1mm. Because the hoisting PLC can only be moved downward if this threshold is exceed, the lag time of the strategic controller is not an issue.

Immediately after the hoisting is lowered 1 mm, the coordinator will overwrite the top drive RPM to an initial value of 300 RPM in the case of no beginning RPM. The hoisting will then be raised at the slowest allowable speed set by the stepper motor limitations in an attempt to ream the hole open.

During competition drilling, however, since the only two scenarios where the bit needs to be raised are during calibration and stick slip mitigation, there is no need to ream the hole. As such, when overpull is encountered, reaming can be dismissed and the upper hoisting position limit can be reset to the current position.

Twist off

Testing showed that the encoder in the top drive that measures torque and RPM feedback is quite accurate, and because of the brake-capability built in the top-drive, reaction times were more than suitable to prevent a twist-off or over-torque beyond the yield torque of the drill-string.

Stick Slip

While twist off could be completely avoided with the top drive encoder, stick slip was still shown to occur, meaning that optimal setpoints were not in place. Thus, stick slip was defined as 75% of the limit of the twist off limit. While this would not cause the top drive brake to engage, remedial action is still implemented.

Once stick slip is identified, the hoisting system is raised 5 mm to lift off bottom so new parameters can be set. The WOB is set to 0.9*old WOB and RPM is increased to 1.1 * old RPM.

Leak

Due to the automation nature of the rig, there is no mitigation for a leak, and thus, this signifies a catastrophic failure which means all systems must be shut off in order to avoid any further damage. When a leak is detected, the coordination system stops, i.e. the pump is stopped, the

rotation is stopped, and the hoisting controller is toggled off and the actuators are raised 5 mm to be get the bit off bottom.

Pack Off

Like a leak situation mentioned above, there is not much our autonomous rig could do if a pack off was detected. However, in the scenario of a pack-off, the hoisting raises and waits 10 seconds. If the stand pipe pressure does not fall after this period, the system shuts off.

Chapter 3 – Theory

Spring Model

$m_1 = \text{mass of drillstring}$

$m_2 = \text{mass of BHA}$

$d_i = \text{dampening coefficient of element } i$

$k_i = \text{stiffness coefficient of element } i$

$u = \text{external force}$

$A_i = \text{cross sectional area of element } i$

$E_i = \text{Young's Modulus of element } i$

$L_i = \text{length of element } i$

$HL = \text{hook load}$

“On the contrary to full-scale drilling operations, it is not possible to assume that the ROP is simply the block velocity because there is a substantial deformation of the power transmission train as a function of the WOB, as we have seen above, and this fact would lead to a spurious estimation of the ROP. It is therefore necessary to utilize the elevation/WOB relationship obtained during calibration to better estimate the actual bit depth as a function of time and therefore the ROP [4].”

This means that a model must be introduced to know the position of the bit precisely and accurately.

Excluding the dampening term, a system with two elements, a drill-string and bottom hole assembly (BHA), subject to an external force u .

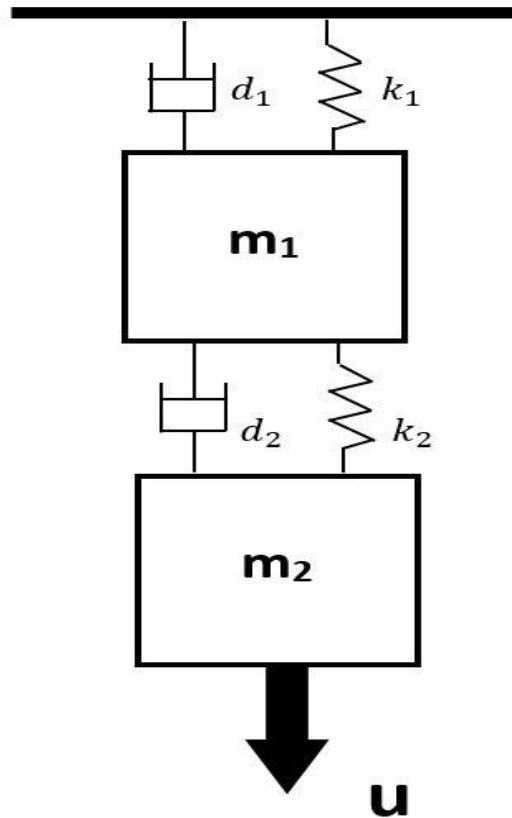


Fig. 3.1: Spring diagram

The force equilibrium equations, excluding the dampening terms, are:

$$u + m_2g - k_2(x_2 - x_1) = m_2\ddot{x}_2$$

$$\ddot{x}_2 = \frac{u}{m_2} - \frac{k_2}{m_2}(x_2 - x_1) + g$$

And

$$m_1g + k_2(x_2 - x_1) - k_1x_1 = m_1\ddot{x}_1$$

$$\ddot{x}_1 = \frac{k_2}{m_1}(x_2 - x_1) - \frac{k_1}{m_1}x_1 + g$$

Where k is the stiffness coefficient and is given by:

$$k_i = \frac{A_i E_i}{L_i}$$

The general form for a spring is:

$$\mathbf{M}\ddot{\mathbf{x}} + \mathbf{D}\dot{\mathbf{x}} + \mathbf{K}\mathbf{x} = m\mathbf{g} + f(u)$$

Where:

$$\mathbf{M} = \begin{bmatrix} m_1 & 0 \\ 0 & m_2 \end{bmatrix}$$

$$\mathbf{K} = \begin{bmatrix} k_1 + k_2 & -k_2 \\ -k_2 & k_2 \end{bmatrix}$$

$$\begin{bmatrix} m_1 & 0 \\ 0 & m_2 \end{bmatrix} \begin{bmatrix} \ddot{x}_1 \\ \ddot{x}_2 \end{bmatrix} + \begin{bmatrix} k_1 + k_2 & -k_2 \\ -k_2 & k_2 \end{bmatrix} \begin{bmatrix} x_1 \\ x_2 \end{bmatrix} = \begin{bmatrix} m_1 \\ m_2 \end{bmatrix} g + \begin{bmatrix} 0 \\ u \end{bmatrix}$$

In order to solve this we need to get the above matrices into the following solvable form:

$$\dot{\mathbf{y}} = \mathbf{A}\mathbf{y} + \mathbf{B}u$$

To deal with only first order differentials, the following rearrangements are made:

$$y_1 = x_1$$

$$y_2 = \dot{x}_1$$

$$y_3 = x_2$$

$$y_4 = \dot{x}_2$$

So:

$$\dot{y}_2 = \ddot{x}_1$$

$$\dot{y}_4 = \ddot{x}_2$$

And:

$$\dot{y}_1 = y_2$$

$$\dot{y}_2 = -\frac{(k_2 + k_1)}{m_1} y_1 + \frac{k_2}{m_1} y_3 + g - \frac{1}{m_1} u$$

$$\dot{y}_3 = y_4$$

$$\dot{y}_4 = \frac{k_2}{m_2} y_1 - \frac{k_2}{m_2} y_3 + g + \frac{1}{m_2} u$$

Where HL is equal to hook load and is given by:

$$HL = (m_1 + m_2)g - u$$

Put into matrix form, this looks as following:

$$\begin{bmatrix} \dot{y}_1 \\ \dot{y}_2 \\ \dot{y}_3 \\ \dot{y}_4 \end{bmatrix} = \begin{bmatrix} 0 & 1 & 0 & 0 \\ -\frac{(k_2 + k_1)}{m_1} & 0 & \frac{k_2}{m_1} & 0 \\ 0 & 0 & 0 & 1 \\ \frac{k_2}{m_2} & 0 & -\frac{k_2}{m_2} & 0 \end{bmatrix} \begin{bmatrix} y_1 \\ y_2 \\ y_3 \\ y_4 \end{bmatrix} + \begin{bmatrix} 0 & 0 \\ 1 & -\frac{1}{m_1} \\ 0 & 0 \\ 1 & \frac{1}{m_2} \end{bmatrix} \begin{bmatrix} g \\ u \end{bmatrix}$$

Note that the external force u , can be rearranged so to be expressed terms of hook load (HL), which is given by:

$$HL = (m_1 + m_2)g - u$$

$$u = (m_1 + m_2)g - HL$$

Cayeux and Skadsmen have shown a similar approach in order to numerically calculate lateral deformations in the x-y plane [4].

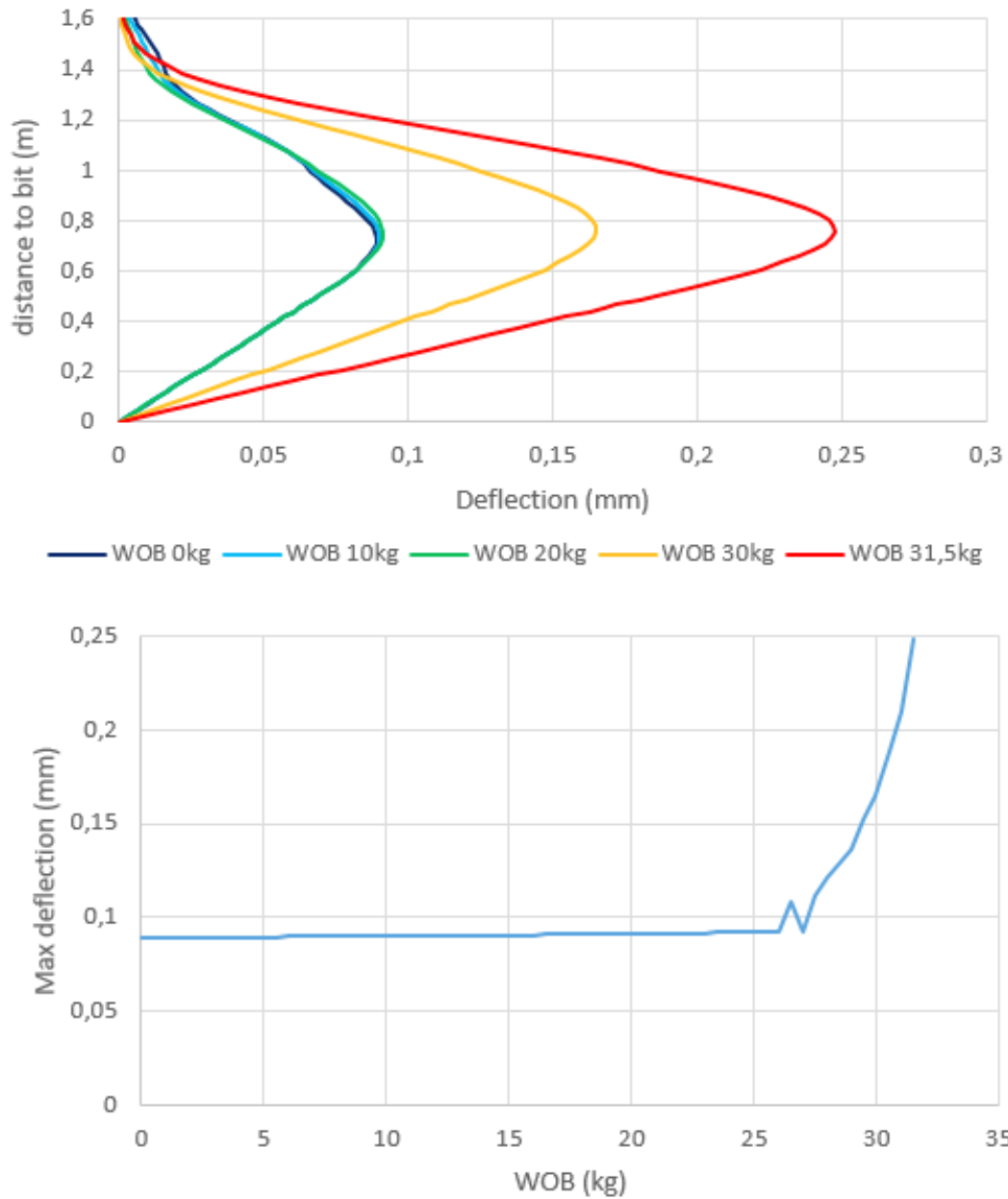


Fig. 3.2: Calculated deformation of a drill-string as a function of the WOB and for an inclination of 3 degrees [4]

Torsional Model

θ_{td} = angle of top drive

θ_b = angle of bit

μ_b = friction coefficient between bottom and bit

μ = friction coefficient between wall and bit

k_i = stiffness coefficient of element i

d_i = internal dampening coefficient of element i

T_i = torque of element i

j_i = inertia of element i

Now that a model has been proposed in the z plane, a model in the x - y plane must be used. Again, we assume a model with two elements, a drill-string and a BHA:

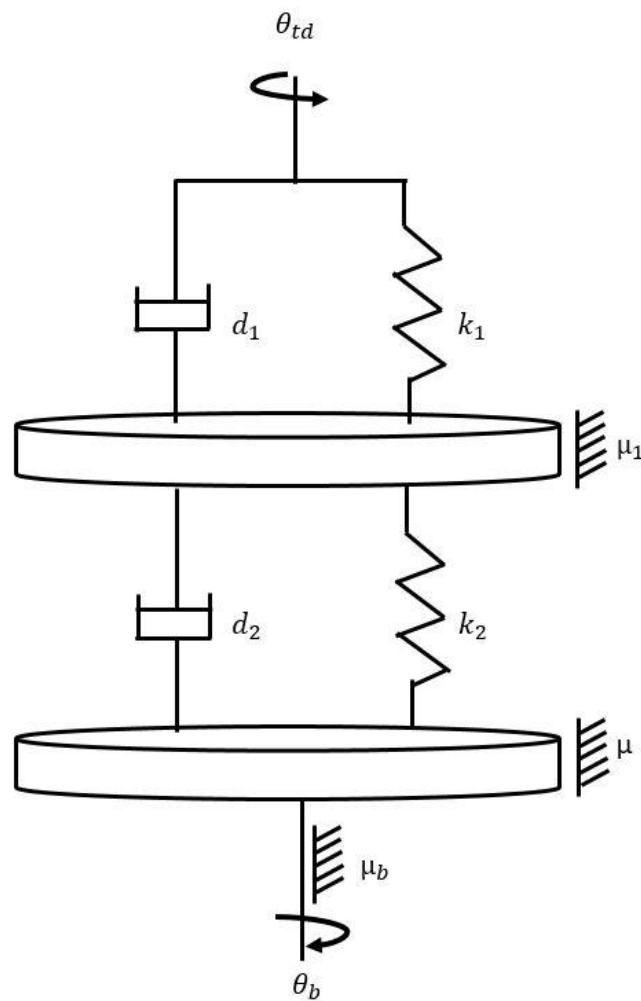


Fig. 3.3: Simplified torsional diagram

The general equation for torque is given as:

$$\tau = j\ddot{\theta}$$

Thus the above systems has the following equations:

$$T_1 - T_2 = j_1 \ddot{\theta}_1$$

$$T_2 - \mu_b \dot{\theta}_2 = j_2 \ddot{\theta}_2$$

$$T_1 = d_1(\dot{\theta}_{td} - \dot{\theta}_1) + k_1(\theta_{td} - \theta_1)$$

$$T_2 = d_2(\dot{\theta}_1 - \dot{\theta}_b) + k_2(\theta_1 - \theta_b)$$

This can be expanded in to:

$$\ddot{\theta}_1 = \frac{1}{j_1} (d_1(\dot{\theta}_{td} - \dot{\theta}_1) + k_1(\theta_{td} - \theta_1) - d_2(\dot{\theta}_1 - \dot{\theta}_b) - k_2(\theta_1 - \theta_b))$$

$$\ddot{\theta}_2 = \frac{1}{j_2} (d_2(\dot{\theta}_1 - \dot{\theta}_b) + k_2(\theta_1 - \theta_b) - (\mu + \mu_b)\dot{\theta}_b)$$

We then make the following substitutions using the same method as described in the spring model section.

$$x_1 = \dot{\theta}_1$$

$$x_2 = \dot{\theta}_b$$

$$x_3 = \theta_{td} - \theta_1$$

$$x_4 = \theta_1 - \theta_b$$

$$\dot{\theta}_{td} = u$$

Thus:

$$\dot{x}_1 = \ddot{\theta}_1$$

$$\dot{x}_2 = \ddot{\theta}_2$$

$$\dot{x}_3 = \dot{\theta}_{td} - \dot{\theta}_1$$

$$\dot{x}_4 = \dot{\theta}_1 - \dot{\theta}_b$$

Substituting these equations back into system equations yield:

$$\dot{x}_1 = \frac{1}{j_1} (d_1(u - x_1) + k_1x_3 - d_2(x_1 - x_2) - k_2x_4)$$

$$\dot{x}_2 = \frac{1}{j_2} (d_2(x_1 - x_2) + k_2x_4 - (\mu + \mu_b)x_2)$$

Thus:

$$\dot{x}_1 = -\frac{1}{j_1} (d_1 + d_2)x_1 + \frac{d_2}{j_1}x_2 + \frac{k_1}{j_1}x_3 - \frac{k_2}{j_1}x_4 + \frac{d_1}{j_1}u$$

$$\dot{x}_2 = \frac{d_2}{j_2}x_1 - \frac{1}{j_2}(d_2 + \mu + \mu_b)x_2 + \frac{k_2}{j_2}x_4$$

In standard matrix formation, the following system matrices are formed, with top drive speed, x_1 , as a measurement.

$$\mathbf{x} = \begin{bmatrix} x_1 \\ x_2 \\ x_3 \\ x_4 \end{bmatrix}$$

$$\mathbf{A} = \begin{bmatrix} -\frac{1}{j_1} (d_1 + d_2) & \frac{d_2}{j_1} & \frac{k_1}{j_1} & -\frac{k_2}{j_1} \\ \frac{d_2}{j_2} & -\frac{1}{j_2} (d_2 + \mu + \mu_b) & 0 & \frac{k_2}{j_2} \\ -1 & 0 & 0 & 0 \\ 0 & -1 & 0 & 0 \end{bmatrix}$$

$$\mathbf{B} = \begin{bmatrix} \frac{d_1}{j_1} \\ 0 \\ 0 \\ 0 \end{bmatrix}$$

$$\mathbf{C} = [1 \ 0 \ 0 \ 0]$$

Using $\mu = 1.0$, the following simulation results are obtained:

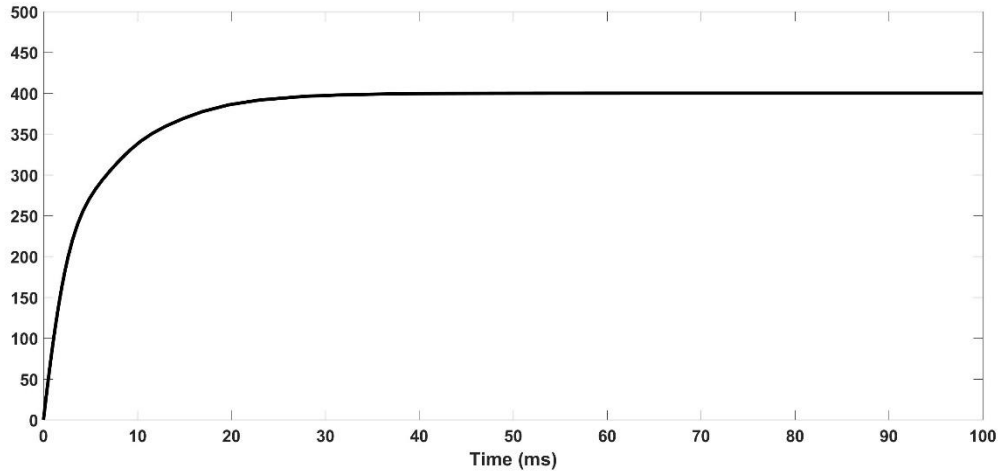


Fig. 3.4: Position of system as function of time

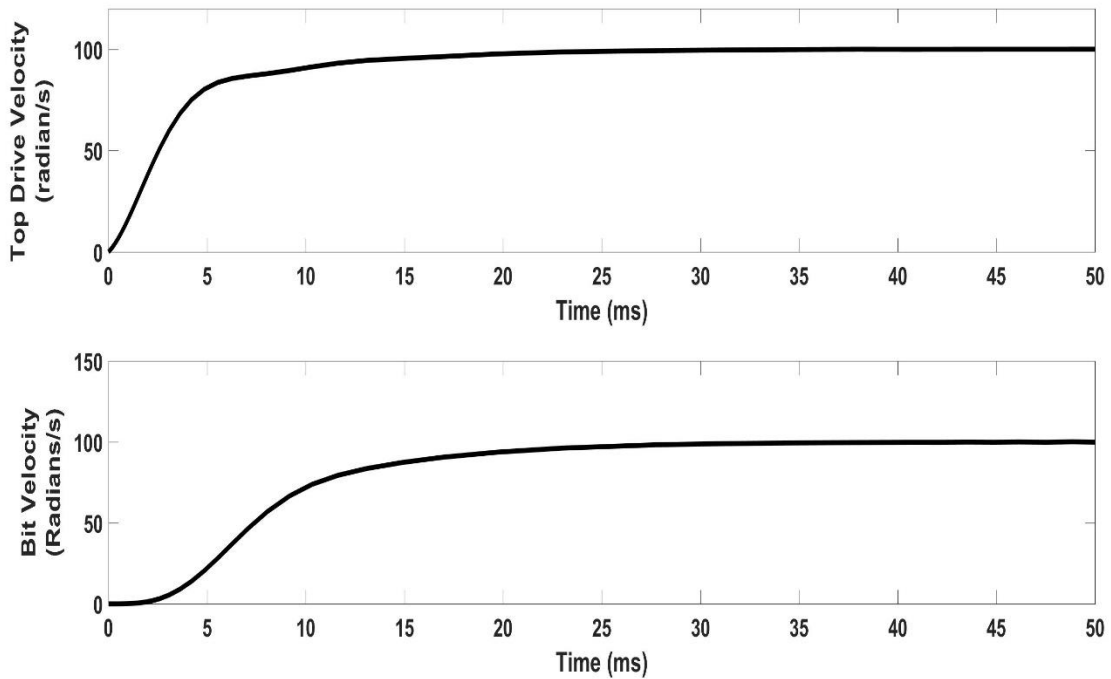


Fig. 3.5: Velocity simulations of both elements

Johannessen and Myrvold have given a generic solution to this model for n number of elements and have shown that this model can be used to simplify a drill-string [5]. However, it should be noted that with increased drilling, the number of states has to be increased accordingly to match the number of elements.

Rate of Penetration

Instantaneous ROP

Rate of penetration (ROP) is defined as the change in bit depth, $dh(t)$, versus the change in time, dt . As such, it is one of the most important factors taking into account cost and efficiency. The mathematical definition of continuous ROP is therefore:

$$ROP(t) = \frac{dh(t)}{dt}$$

Applying Euler's method to the above equation gives:

$$h(t + 1) = h(t) + ROP(t) * \Delta t$$

Where delta t is the sampling instance. With the help of Kalman filter, discussed more in chapter 4, the instantaneous ROP value can be calculated based on the depth measurement with the following assumption [6]

$$ROP(t + 1) = ROP(t) + w(t)$$

Where w is the disturbance term associated with the fluctuation of the ROP. Combing the equations gives a 2 dimensional system

$$h(t + 1) = h(t) + ROP(t) * \Delta t$$

$$ROP(t + 1) = ROP(t) + d(t)$$

The measurements of bit depth can be transmitted and logged real time and the instantaneous ROP can be estimated using a similar 2-dimensional system as described further above via Kalman filter or other filtering technology [6]

Empirical ROP Model

“It has been shown that ROP can be modeled as a nonlinear function dependent on several drilling parameters such as formation strength, compaction, bottom hole pressure differential, flow rate, WOB, RPM, bit diameter, tooth wear and bit hydraulics [7].” The following is the Bourgoyne-Young ROP model

$$ROP = e^{(a_1 + \sum_{i=2}^8 a_i x_i)}$$

Where x_i is the known data that is dependent on drilling parameters and drilling fluid properties, and a_i are the variable coefficients. The coefficients are as follows.

- X1 represents the formation strength.
- X2 = TVD – current depth
- X3 represents the increase in pore pressure and is equal to $D^{0.69}(p_p - 10.5)$
- X4 represents the differential pressure and is equal to $D(p_p - p_c)$. This equation describes exponential decrease of drilling rate with the bottom pressure overbalance. X4 is equal to 1 when there is no overbalance
- And X5 to X8 can be taken to be negligible

Drilling Optimization

Founders Point

Eric Cayeux et. al [8] has shown that ROP has a linearly relationship between RPM and WOB. This means that the optimal ROP is the point at which ROP diverges away from a linear relationship.

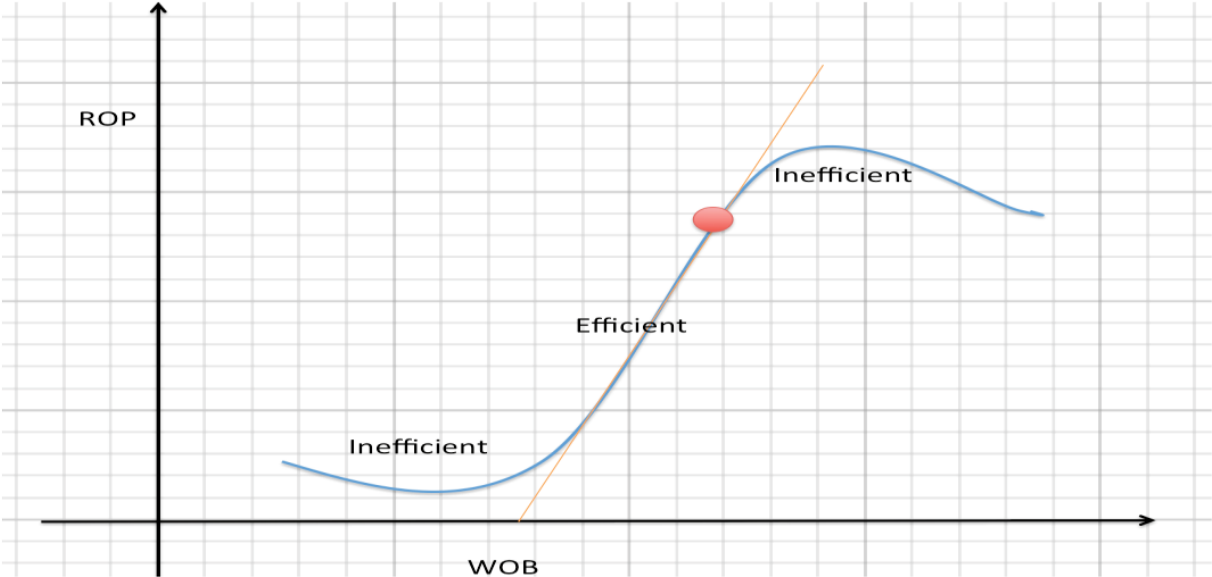


Fig. 3.4: Linear relationship of WOB and ROP [1]

The founders point determined by the formation/rock type, and thus if a new formation is detected, then a new optimal RPM and WOB parameter combination must be found. This is accomplished by sweeping the WOB and RPM values to find a “sweet spot” for ROP.

Sweeping

In order to find these “optimal parameters” a sweep of WOB and RPM must be performed. This entails gradually increasing the WOB and RPM in steps in then comparing the new ROP to the previous ROP.

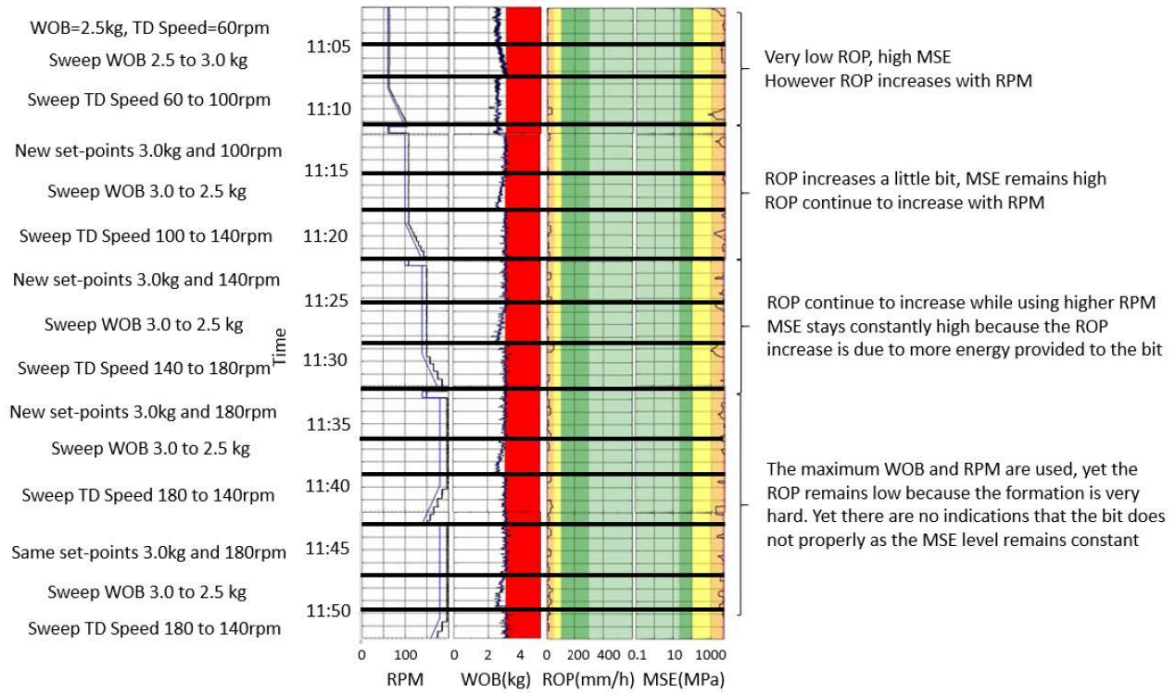


Fig. 3.5 Results from last year's rig sweeping algorithm. Note that their rig had a maximum limit of 3 kg WOB and 180 RPM [8]

New Formation Detection

After a sweep has been performed, the WOB and RPM setpoints remain will remain constant. Thus, a method needs to be introduced in order to give the system an idea of when to re sweep for new optimal parameters. The obvious solution would be to do this once a new formation has been encountered, and thus, a way to detect a new formation is required.

MSE, or the mean specific energy, is a measure of how much energy it takes to remove a material [3].

$$MSE = \frac{\text{Energy Input}}{\text{Removed Volume}}$$

Todd Robert Hamrick [3] and Olaleke Akisanimi [9] have shown how to convert this to bit torque, RPM, ROP, bit diameter and WOB.

$$MSE = \frac{4 * \tau_{bit} * \dot{\omega}_{bit}}{\pi * v_{bit} * d_{bit}^2} + \frac{4 * WOB}{\frac{\pi}{4} * d_{bit}^2}$$

In order to compare this to rock strengths, the MSE must be converted to the unconfined compressive strength (UCS).

UCS

UCS, or unconfined compressive strength is a measure of a materials strength.

“Even if no sensors are implemented to perform any kind of well-logging before the formation is encountered during drilling, the rig surveillance has been programmed to calculate the approximate UCS [MPa] for formations, based on bit-torque and ROP-calculations. UCS values that range between 10 and 100 MPa typically have a friction factor that can be expected to range from 0.84 and 0.93. Because the exact UCS of the rock samples generally are unknown, the bit-torque in early experiments will be calculated with an approximate friction factor of 0.885 [8]”

From this paper, this leads to the following equation [10]

$$UCS \approx \frac{\ln\left(\frac{\tau_{bit} * 36}{0.9402 * WOB * d_{bit}}\right)}{1.16 * 10^{-9}}$$

This UCS can be used to classify the rock strength of the material being formed and thus give some idea to what type of rock is present. Below is a summary of the strength classification and associated rock types [11]

Table 3.1: Strength Classification of various rock types and UCS values

Strength Classification	UCS [MPa]	Typical Rock Types
Very Weak	10 - 20	Weathered and weakly compacted sedimentary rocks
Weak	20 - 40	Weakly cemented sedimentary rock
Medium	40 - 80	Competent sedimentary rocks; some low-density coarse grained igneous rocks
Strong	80 - 160	Competent igneous rocks, some metamorphic rocks and fine-grained sandstones
Very Strong	160 - 320	Quartzites, dense fine-grained igneous rocks

Chapter 4 - Control Systems and Data Acquisition and Handling

Filters

Median Filter

Due to heavy electromagnetic interference from the other systems, the sensors had extreme levels of noise an undetermined low frequency (estimated between 30 and 100 Hz). Due to lack of time, these spikes were filtered out using a median filter.

Low Pass Filter

Throughout this project, a standard first order low pass filter is applied to the data to filter out sensor noise. The basic procedure for doing so is outlined below.

The number of data samples (N) must be taken to a power of two, (i.e. $2^8 = 256$ data samples). Next, the domain data is converted into frequency domain using a Fast Fourier Transformation (FFT). The frequency axis is thus

$$W = W_s \left[-\frac{N}{2}, \frac{\left(\frac{N}{2} - 1\right)}{N} \right]$$

Where W_s is the sampling frequency (≈ 37 samples/minute for the circulation PLC).

Next, the amplitude of FFT data vs frequency is plotted with the goal of identifying the high frequency range that needs to be cut off.

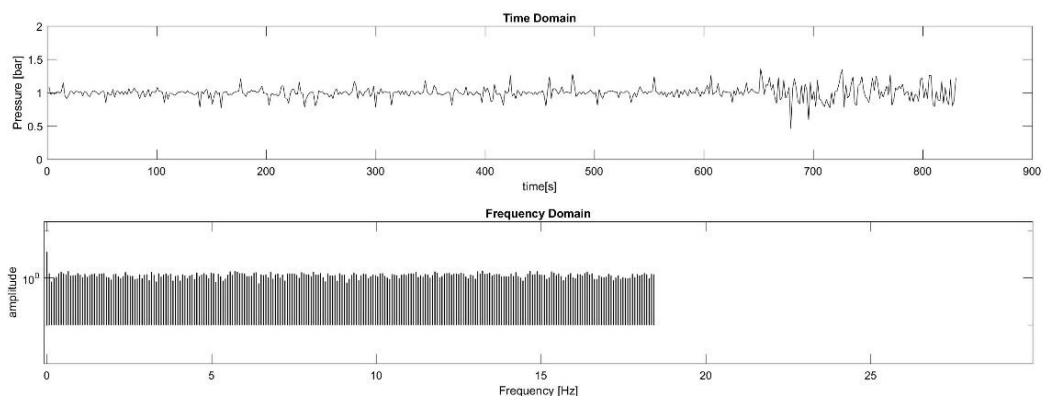


Fig 4.1: Transformation of time domain into frequency domain

Because there are not two distinct bumps in this plot, the cutoff frequency must be decided with a different method as it is clear some filtering is required. Thus, a trial and error method was used to

manually set the cut off frequency. Below is a graph of WOB before and after applying a low pass filter that was calculated using the same method.

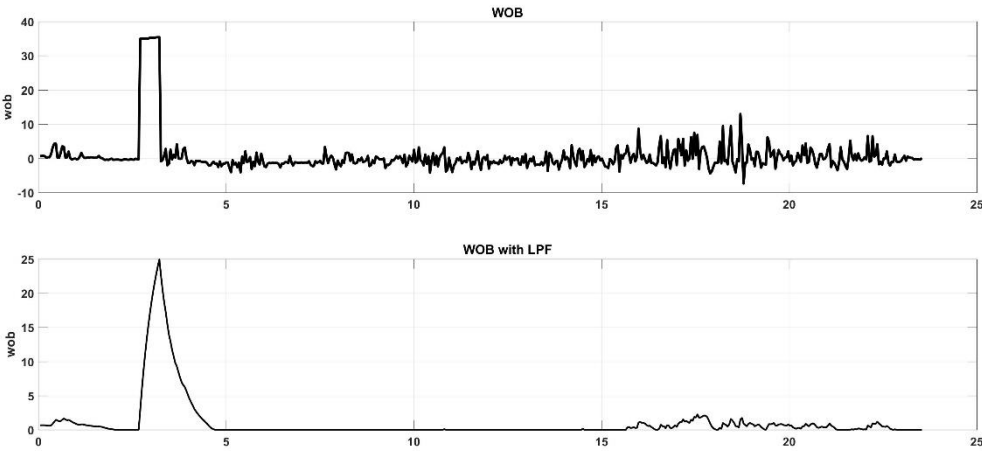


Fig 4.2: Low pass filtering of WOB data

Control Systems

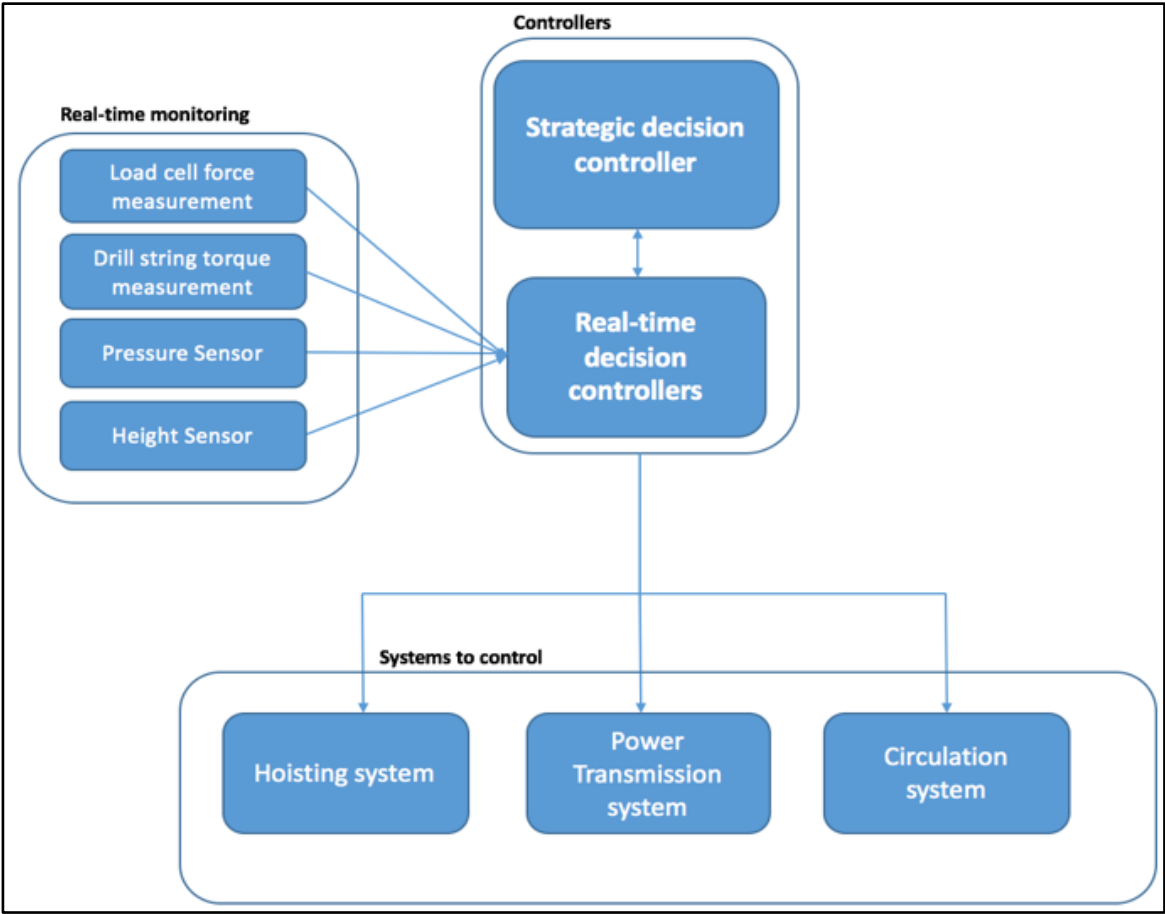


Fig 4.3: Control hierarchy of the rig

Open Loop vs Closed Loop Systems

An open-loop controller is often used in simple processes because of its simplicity and low cost, especially in systems where feedback is not critical. A typical example would be a conventional washing machine, for which the length of machine wash time is entirely dependent on the judgment and estimation of the human operator. Generally, to obtain a more accurate or more adaptive control, it is necessary to feed the output of the system back to the inputs of the controller. This type of system is called a closed-loop system ([Wikipedia](#)).

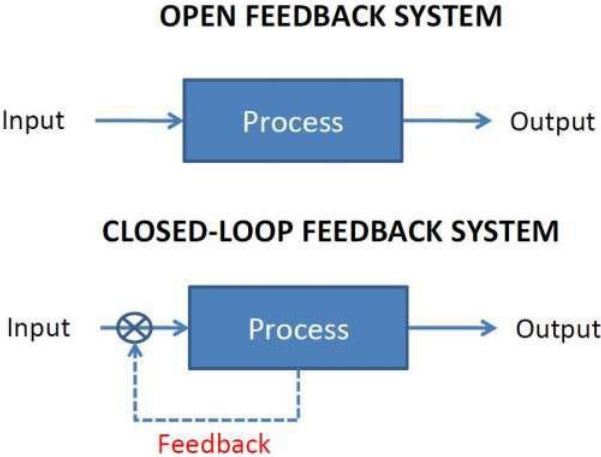


Fig 4.4: Open loop vs Closed loop feedback system [12]

“In a simple schematic of the control system, the input drives the controller. Most controllers are model-based and computer-based. Output values can be measured from the process system. This system includes a feedback loop, which feeds the output values back to the controller to adjust the controller output, making it a closed-loop control system [6]”.

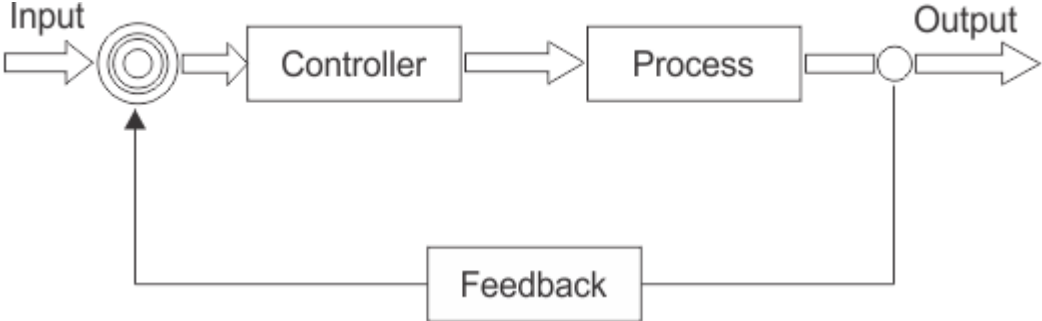


Fig. 4.5: A common feedback system [6]

A proportional-integral-derivate (PID) controller is one such control loop feedback controller commonly used. It calculates an error value $e(t)$ as the difference between a desired setpoint and a measured process variable and applies a correction base on proportional, integral and derivate terms, as shown below [13].

$$u(t) = K_p e(t) + K_i \int_0^t e(\tau) d\tau + K_d \frac{de(t)}{dt}$$

For our purposes, as is for many applications, the derivative term was excluded as it causes too much fluctuations. Through much trial and error, good proportional and integral coefficient gains were found to be both 0.00001.

The following diagram is the incorporation of these filters, feedback system, and PID controller that were implemented on the rig.

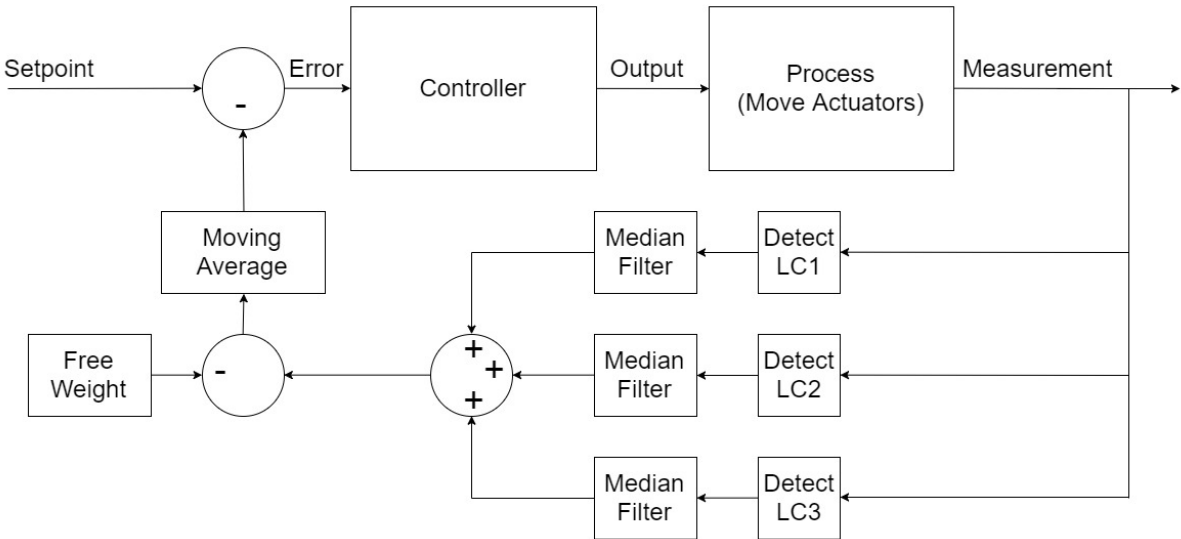


Fig. 4.6: Hoisting block diagram

While this setup gave sufficient control of the hoisting system, it is proposed that further research be done in incorporating a model based feedback system.

Kalman Filter

A Kalman filter, or linear quadratic estimation (LQE), is a model based approach that compares a measured value to predicted output that adjusts the controller accordingly. This is generally a “smarter” design than the above-mentioned system, and yields more accurate results. As such, this is a common technique used in aircraft and guidance control.

Below, a system is proposed for a more advanced system that can predict the outputs with some event horizon.

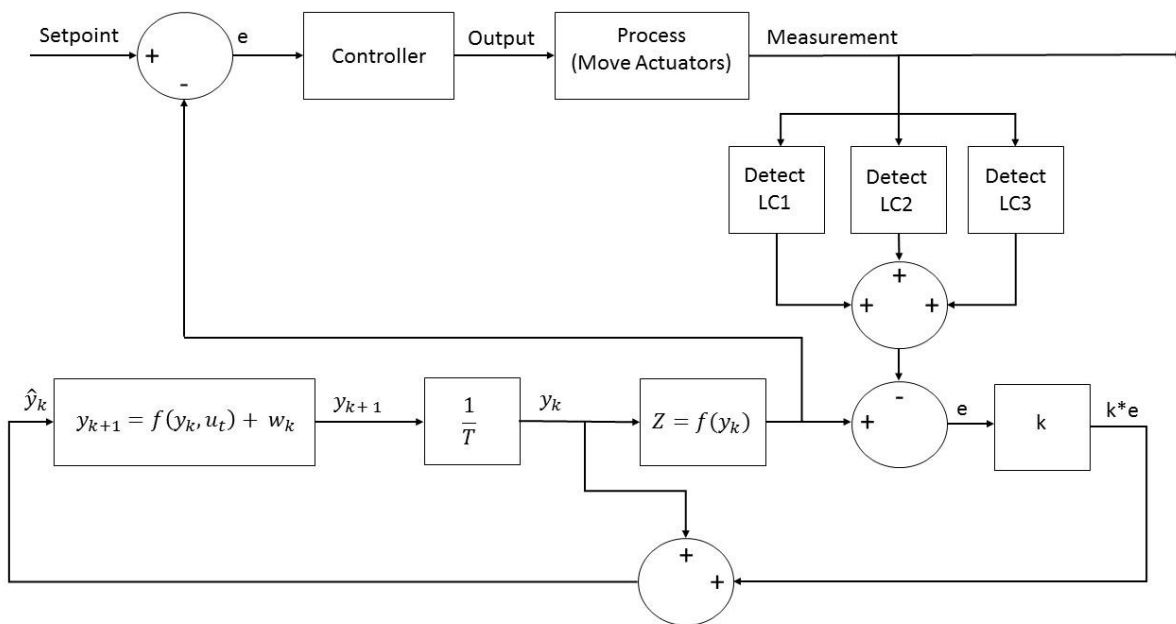


Fig 4.7: Proposed block diagram implementing a Kalman filter

Automation Tools

Tools: Computer is used to process/analyze the data and provide process control action.

Tools: Data acquisition system is the process of sampling signals that measure real world physical conditions and converting the resulting samples into digital numeric values that can be manipulated by a computer. The components of data acquisition systems include:

- **Sensor** (transmitter) measures physical parameters, like level, pressure, temperature, flow rate, force, velocity, displacement, acceleration, strain, etc. It converts physical parameters to electrical signals.

Calibrating Load Cells

Each load cell was calibrated using a precise lab scale for various weights. Below is an example of one of the load cells.

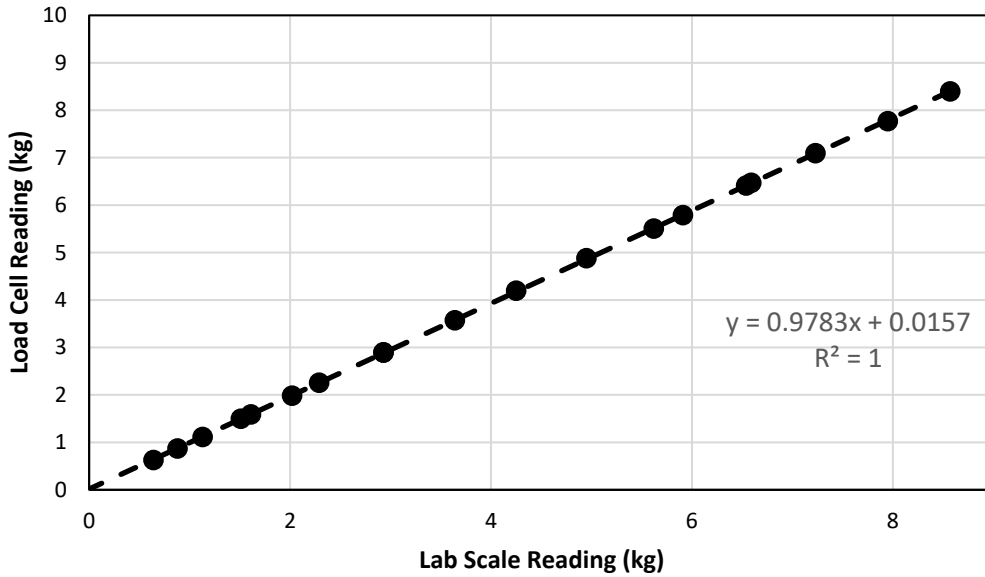


Fig 4.8: Calibration of load cells

- **Analog-to-digital converters**, to convert conditioned sensor signals to digital values.

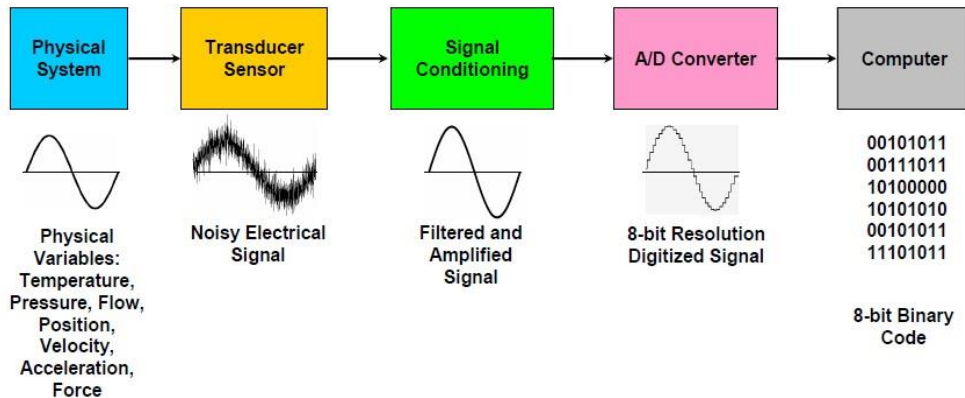


Fig. 4.9: Process of ADC [14]

- **Digital-to-analog converters**, to convert digital signals into an analog output

Simple Equation of Pressure

The pressure sensor outputs 4 – 20 mA linearly corresponding to a pressure range of 0 – 10 barg. Using a 220 ohm resistor to control the voltage range and ohms law, this corresponds to a range of 0.88 to 4.4 volts:

$$V = I * R$$

$$V = 4 \text{ mA} * 220 \Omega = 0.88 \text{ Volts}$$

$$Pressure (barg) = \left[\left(\frac{integer * \left(\frac{3.3 V}{1024} \right) * 1000}{220 \Omega} \right) - 4 mA \right] * \frac{10 mA}{16 mA}$$

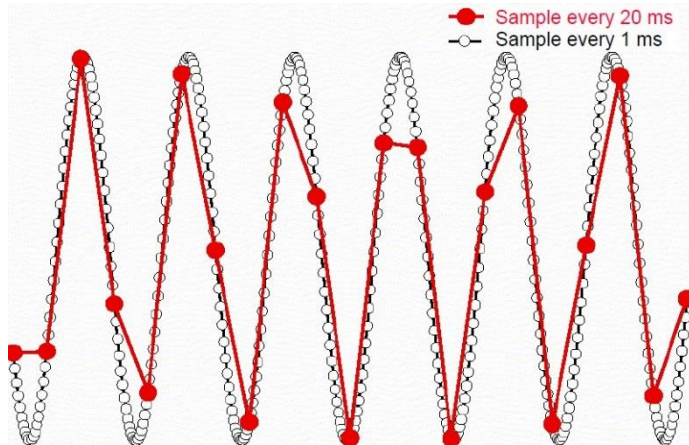


Fig. 4.10: *Effect of data sampling rate [14]*

Tools: A Programmable Logic Controller, or PLC, is more or less a small computer with a built-in operating system (OS). This OS is highly specialized and optimized to handle incoming events in real time, i.e., at the time of their occurrence. The PLC has input lines, to which *sensors* are connected to notify of events (such as temperature above/below a certain level, liquid level reached, etc.), and output lines, to which *actuators* are connected to effect or signal reactions to the incoming events (such as start an engine, open/close a valve, and so on) ([Wikipedia](#)).

Speed

Eric Cayuex has shown that as loop times increase, the drilling limits are decreased for a similar drill-string and BHA [8].

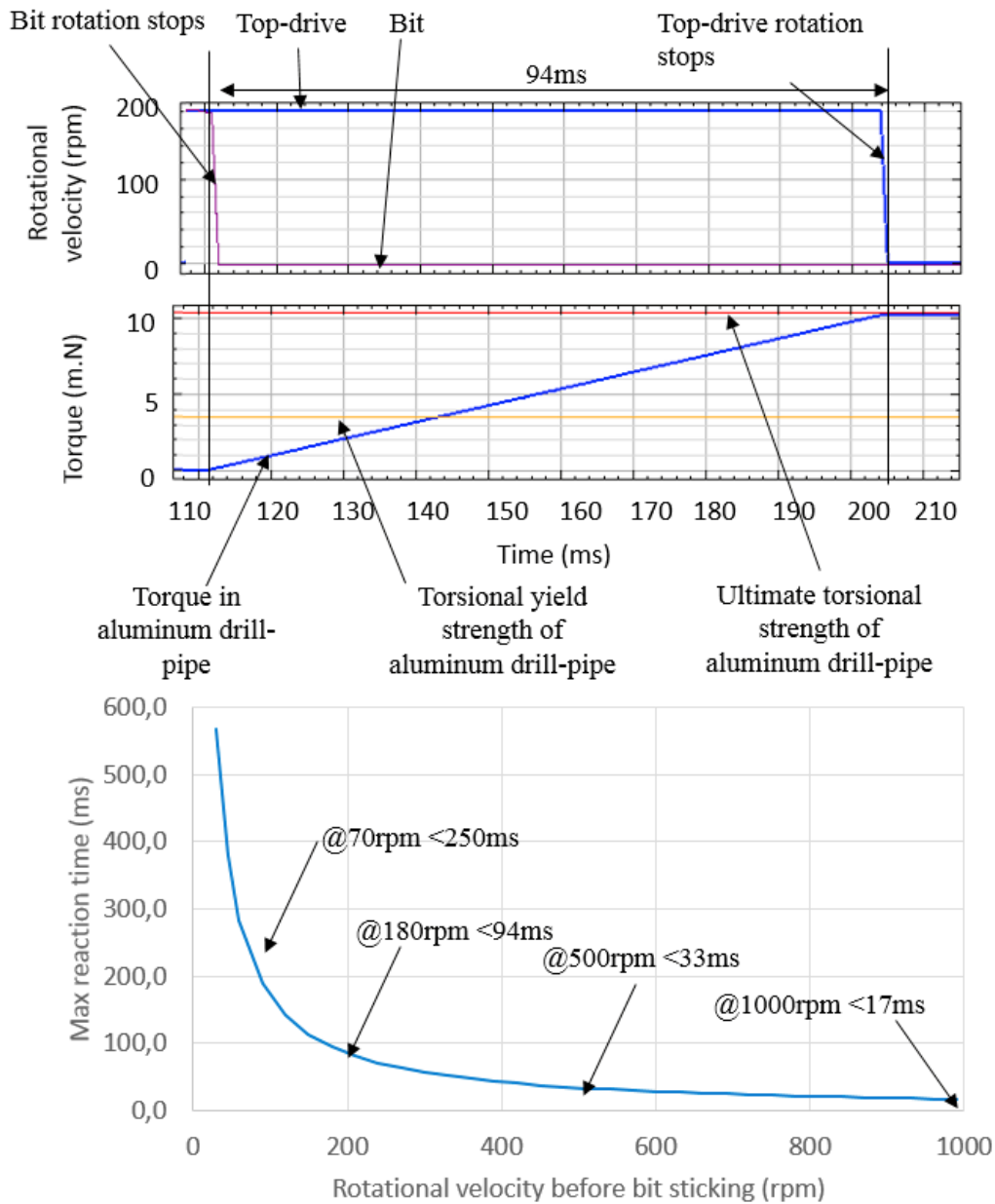


Fig. 4.11: Loop times on a similar drill-string [8]

For instance, if the PLC has a 33 ms loop time, then approximately 500 RPM is achievable.

However, if the loop time is tripled to approximately 94 ms, then the highest achievable RPM is 180. This demonstrates the importance of efficient coding of the PLC. Below are examples of how important loop time is on the system.

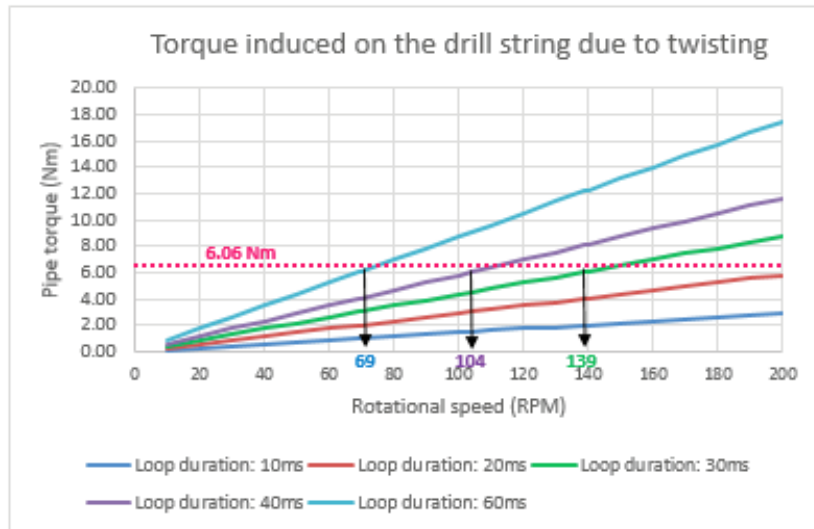


Fig. 4.12: Twist torque as a function of initial rpm for different loop durations [9]

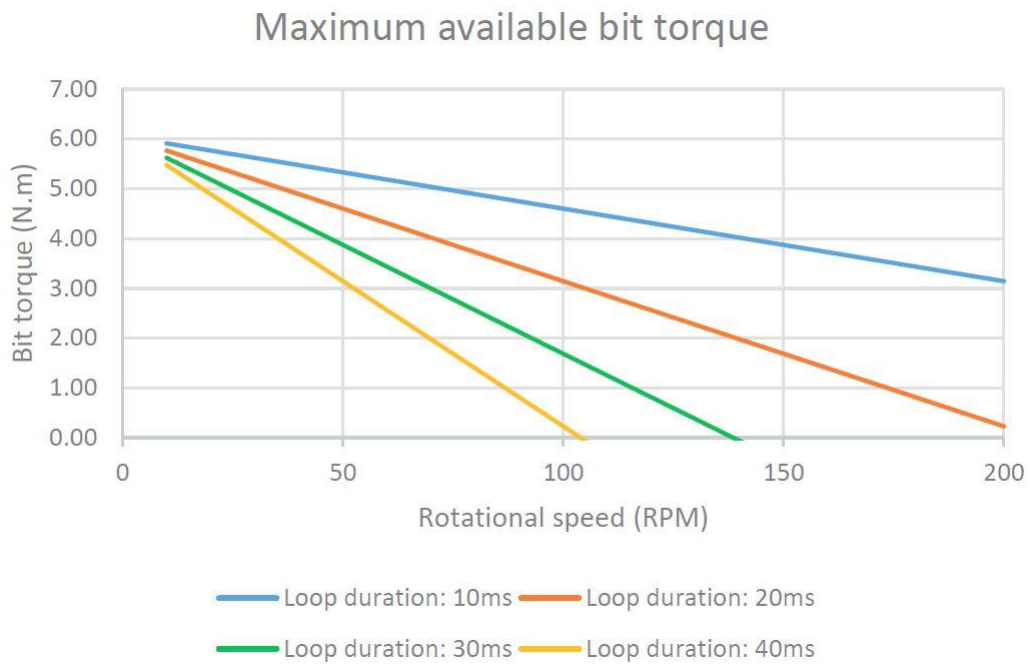


Fig 4.12: Maximum available bit torque as a function of the rpm different loop duration [9]

Loop times also limit the maximum WOB, as it requires a certain time to react to.

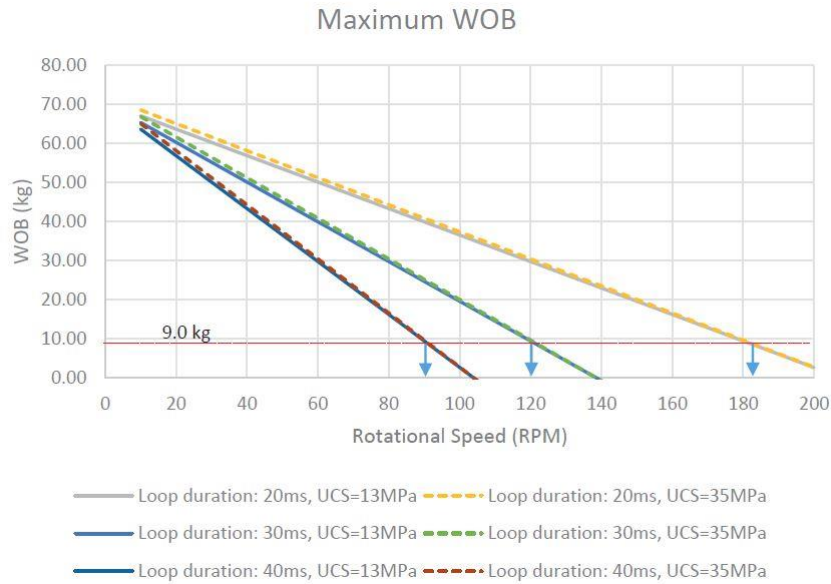


Fig. 4.13: Maximum WOB as a function of the rotational speed for three different control loop durations and two formation hardness [9]

Tools: Human machine interface (HMI) is a software application that gives the purpose of presenting information to the user as well as offering some control of the process, be it alerts, confirmations, or requests to the user about the current state of the process, Typically, information is displayed in a graphic format (Graphical User Interface or GUI) [6].

During the work with the operator, the designer should get an overview of what information is critical for the operator to complete his tasks. It is important to make the important information stand out [6].

The design of the HMI and GUI was built from the ground up to only include what was necessary at the time. Over time, it was adapted to show current systems operations, alert notifications, pertinent sensor information in the form of text and plots as well as providing an interface to manually control each individual system.

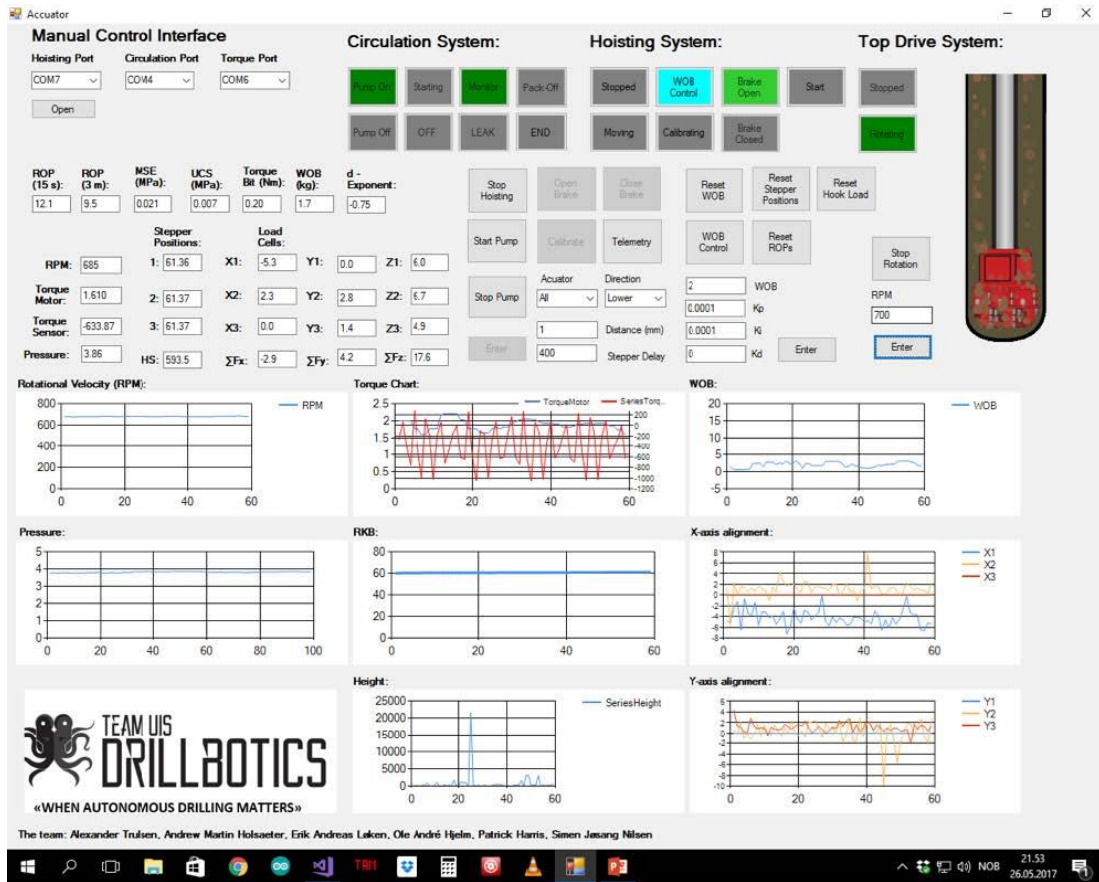


Fig. 4.14: HMI/GUI of the drilling rig

Tools: Database

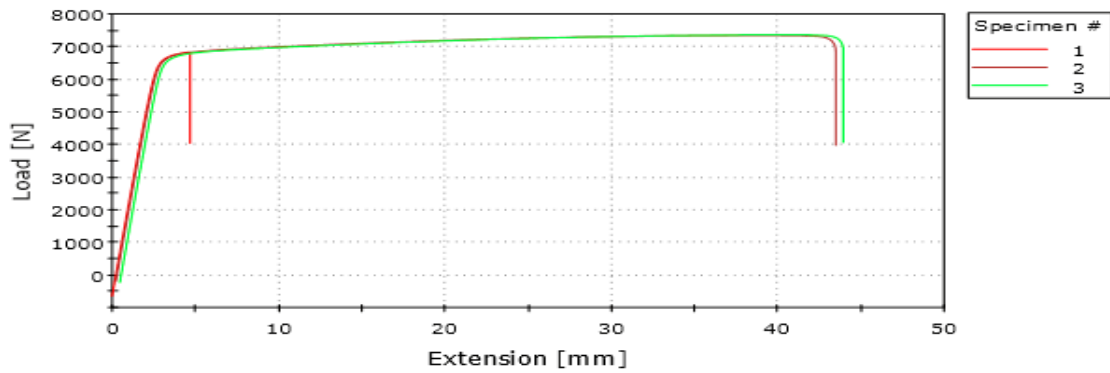
It is of benefit to log all data for analysis so that it can be evaluated and analyzed for future use. A cloud based database was implemented for this reason. It logged all sensor information as well as several important setpoints along with the corresponding time stamp in relation to the computer. This data could then be downloaded in several formats including .csv and .xls to be further analyzed at any time.

Chapter 5 – Experimental Results

Torque

Destruction Testing

Specimen 1 to 3



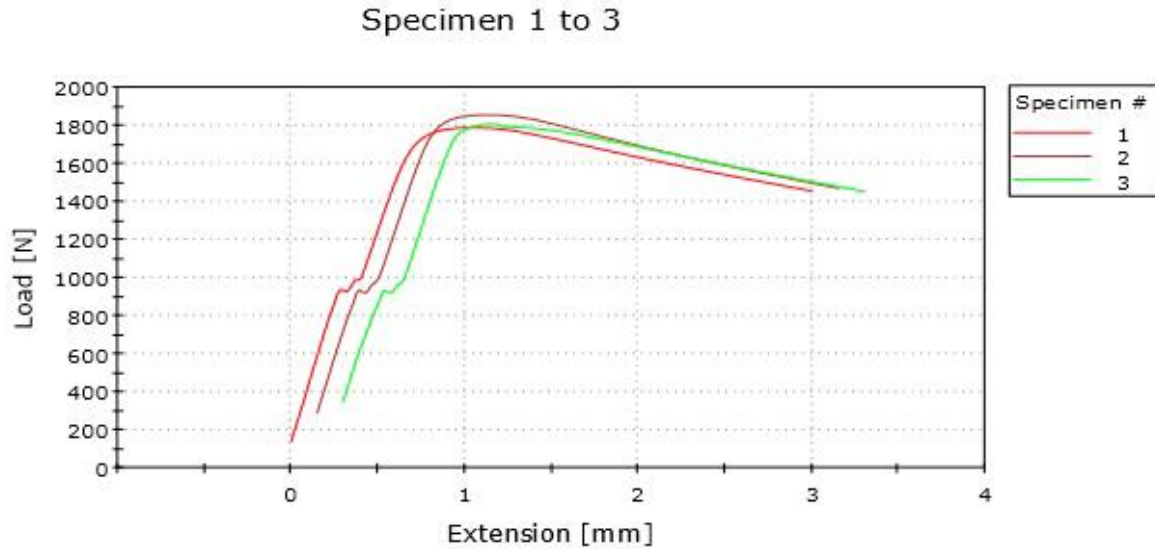
	Specimen label	Max Load [N]	Stress at Max Load [MPa]
1	Test□	6835	283.2
2	Test□	7344	304.3
3	Test□	7360	305.0

	Strain at Max Load [mm/mm]	Stress at □ea□ [MPa]	Strain at □ea□ [mm/mm]
1	0.00726	192.0	0.00731
2	0.06043	197.7	0.06747
3	0.06232	201.8	0.06782

	Extension at Maximum Load [mm]	Tensile stress at Yield (Zero slope) [MPa]	Tensile strain (Extension) at Yield (Zero slope) [mm/mm]
1	4.648	-----	-----
2	38.67	304.3	0.06043
3	39.88	305.0	0.06232

	E-Modulus [MPa]
1	71700
2	71650
3	72200

Fig. 5.1: Tensile test results for an aluminum pipe with 0.035” thickness



	Specimen label	Modulus (E-modulus) [MPa]	Compressive stress at Yield (Zero slope) [MPa]
1	Test-1	51350	74.05
2	Test-2	50690	76.81
3	Test-3	46880	74.80

	Compressive stress at Maximum Load [MPa]	Compressive strain (Extension) at Maximum Load [mm/mm]	Compressive strain (Extension) at Yield (Zero slope) [mm/mm]
1	74.05	0.00163	0.00163
2	76.81	0.00152	0.00152
3	74.80	0.00133	0.00133

	Maximum Load [N]	Extension at Maximum Load [mm]
1	1787	1.046
2	1854	0.97262
3	1805	0.84933

Fig. 5.2: Compressive test results for an aluminum pipe with 0.035" thickness

The strength of the total assembly (drill pipe and BHA) is limited by the strength of the weakest component, the aluminum drill pipe (DP), specified to be used in the competition guidelines (DSATS Drillbotics Guidelines, 2017). In this section, all calculations are related to the aluminum pipe with a wall thickness of 0.035". Aluminum, in its purest form, has an ultimate tensile strength (UTS) of 89 MPa and a yield strength (YS) of 34 MPa. The assumption is made based on "Sheasby et. Al., 2001." Thus, $YS_{max} = 89$ MPa, Ultimate shear stress (USS) = $0.65 \times YS_{max}$, 57 MPa.

Thus, the maximum torque that can be applied before the pipe shears is:

$$\tau_{max} = \frac{USS}{r} * \frac{\pi}{32} * (d_o^4 - d_i^4) = 3.14 Nm$$

And with a safety factor of 1.1:

$$\tau_{max} = 2.854 Nm$$

The maximum applicable torque that can applied before yielding is:

$$\tau_{yield} = \frac{YS}{r} * \frac{\pi}{32} * (d_o^4 - d_i^4) = 1.873 Nm$$

And with a safety factor of 1.1:

$$\tau_{yield} = 1.702 Nm$$

Calculating the critical buckling force as follows

$$Critical\ Buckling\ Force = \frac{(\pi^2 E_y J_z)}{(kL)^2} = 218\ N\ pinned, 26.7\ N\ swaring$$

“In our case, the drill-pipe is pinned to the BHA and the top drive, but we need to account for lateral movement when drilling commences. Good drilling practice can minimize this effect by ensuring maximum ow rate and RPM, combined with a low WOB applied before commencing drilling” [8].

Bit Torque Calculations

Because we are measuring torque of the top drive motor and not the bit torque, a correction factor must be applied. This was done by measuring the motor torque at various RPM’s via the encoder without the drill-string attached, in order to establish a baseline for bit torque to be calculated.

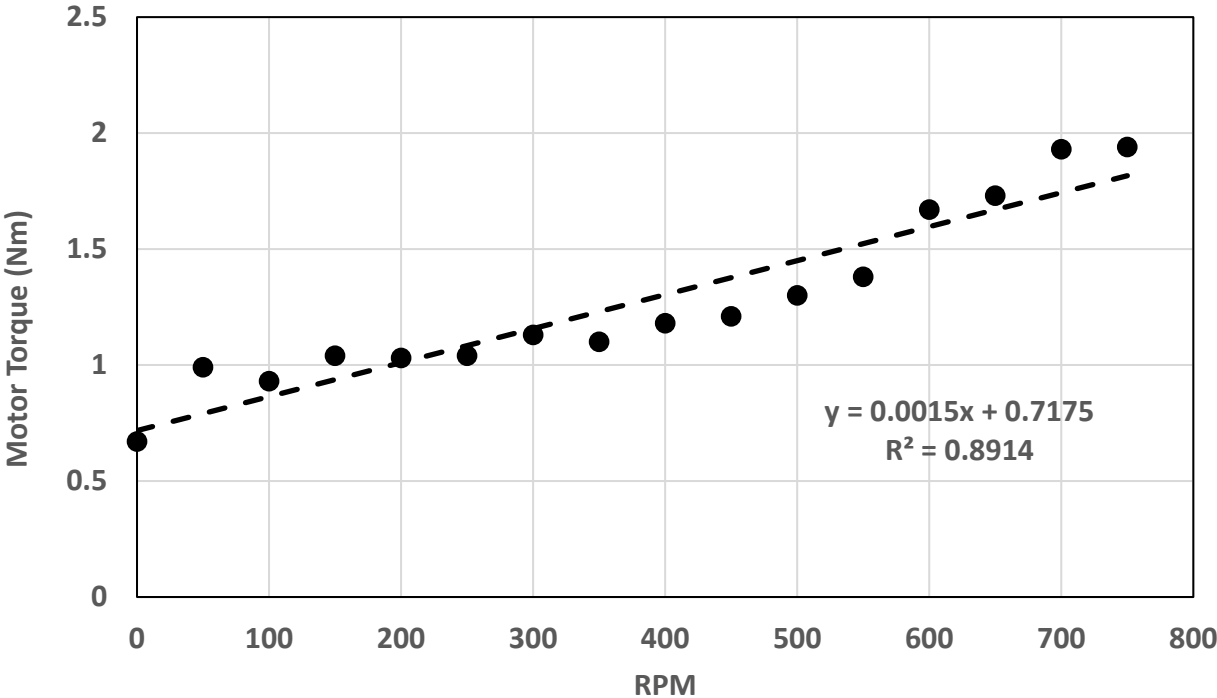


Fig. 5.3: Torque of motor vs RPM

Thus, during real time drilling, bit torque can be calculated as:

$$\tau_{bit} = \tau_{motor} - ((0.0015 * RPM) + 0.07175)$$

Drilling

For testing, two primary rock samples were used. One consisted of mixed cement and the other contained layered hardened tiles consisting of marble, limestone, and other extremely hard material with a dipping angle of 45 degrees.

Note that because constant loop times were not implemented at the time of this drilling, data was stored whenever a new piece of data was received, regardless of the time it came. Thus, the data had to be interpolated so as to compare data for the same time stamp.

Cement

First, a test was carried out to determine the relationship between stepper movement and WOB. After tagging bottom, the hoisting top plate was sent down 0.04 mm at a time (10 steps) and the load cell readings were recorded. The WOB was then calculated as following.

$$WOB = \text{Free Hanging Load} - \sum_{i=1}^3 F_{zi}$$

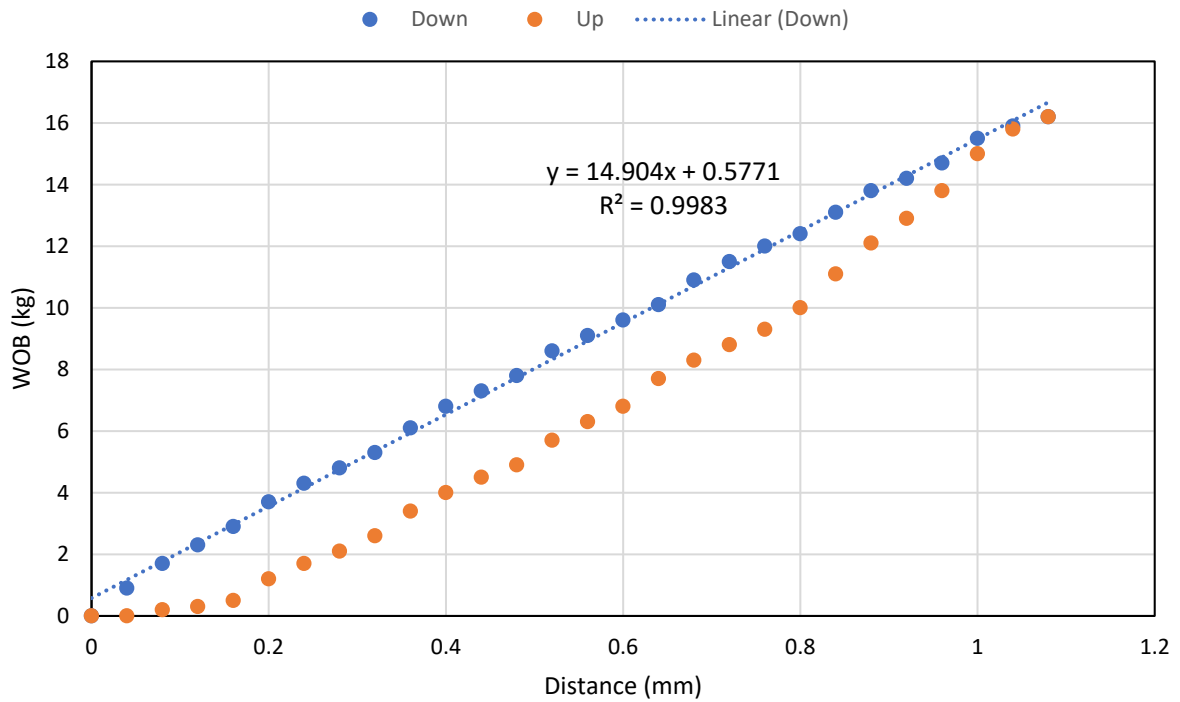


Fig. 5.4: WOB vs distance moved on a cement test sample

As you can see, the WOB vs stepper movement relationship is quite linear with an R^2 value of 0.9983 when applying WOB (moving downward). This energy gets released quickly after initially lifting, and then a linear relationship is reestablished after some distance.

ROP values were filtered and the beginning ROP spike is due to tagging bottom.

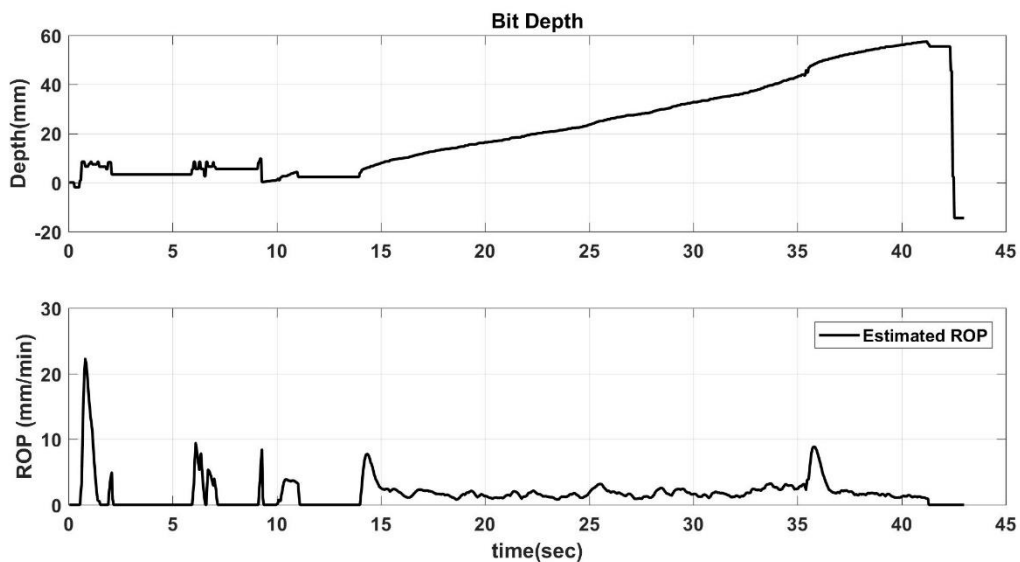


Fig. 5.5: Position and ROP values of drilling through cement

Bit depth and ROP values were filtered.

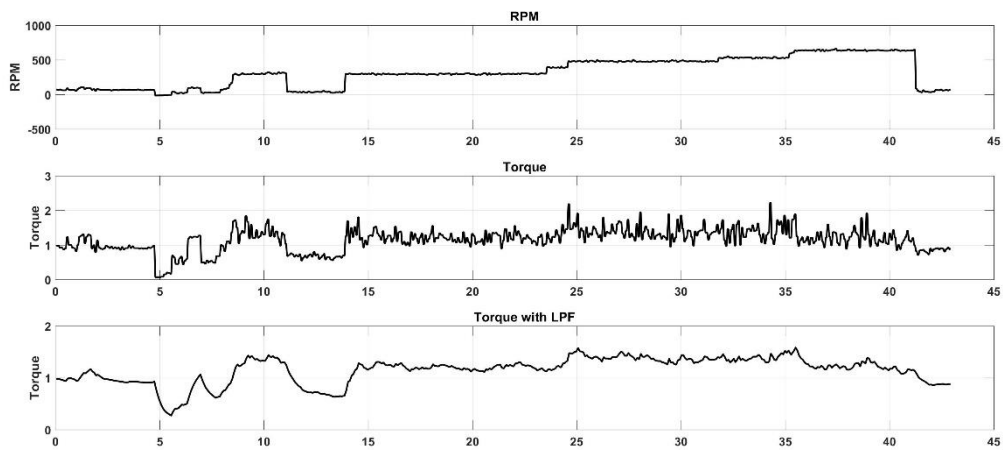


Fig. 5.6: *Data from cement drilling*

The torque data was filtered using a standard first order low pass filter, as was the WOB data below from the same time sample.

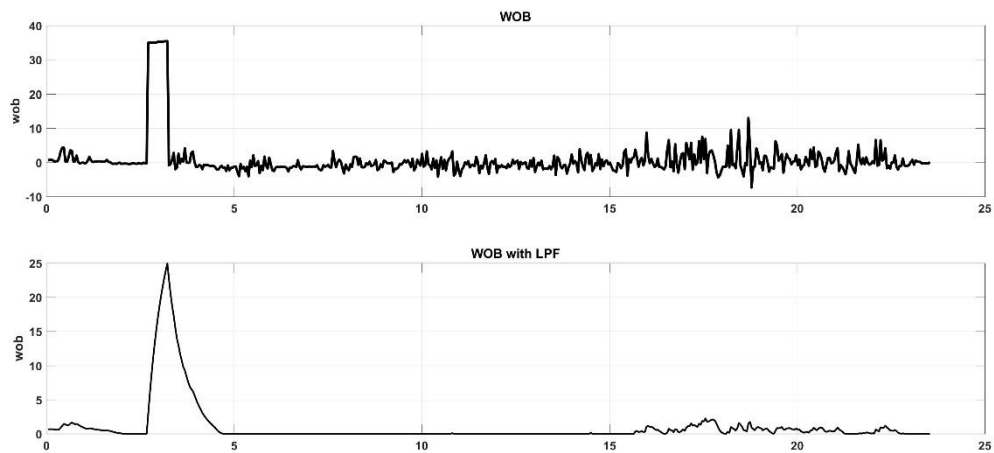


Fig. 5.7: *WOB when drilling cement*

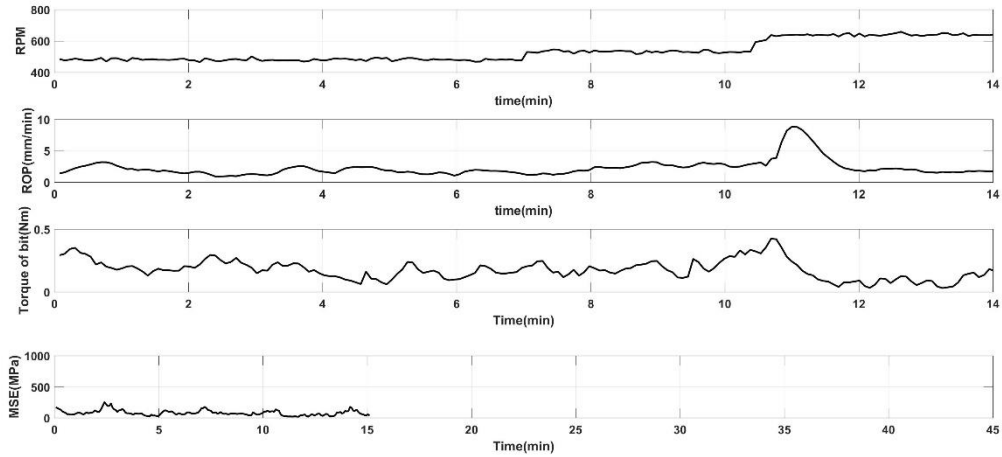


Fig. 5.8: *Drilling data from cement drilling*

MSE/UCS results were only able to be calculated when there was a stable WOB. Thus, only the first 15 minutes yielded results for MSE/UCS values.

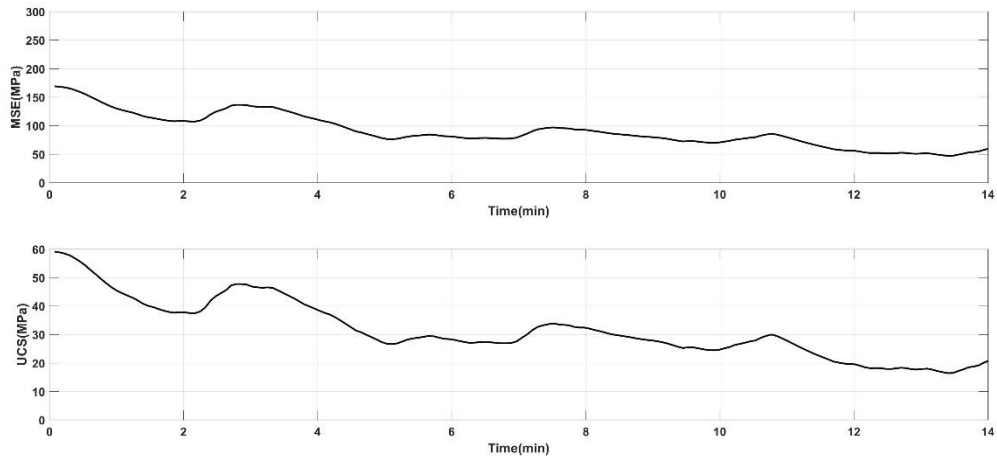


Fig. 5.9: *Filtered MSE and UCS data for drilling cement*

From the above graph, a UCS in the range of 25 – 50 is calculated. According to Table 3.1, this corresponds to a rock strength of weak to medium which makes sense for cement.

Tiles

Drilling data was taken from a sample drilling time of 30 minutes. Due to the hardness of the tiles, the maximum ROP was significantly lower than that of cement with similar drilling setpoints.

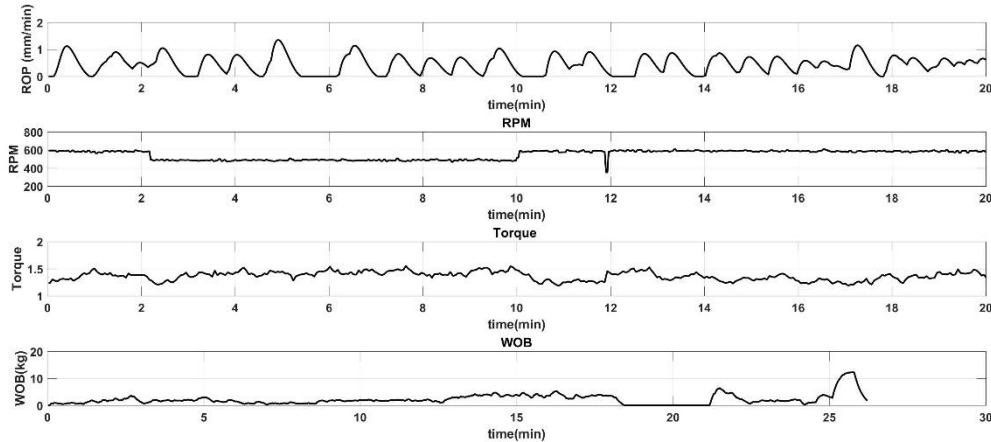


Fig 5.10: Raw drilling data for tiles

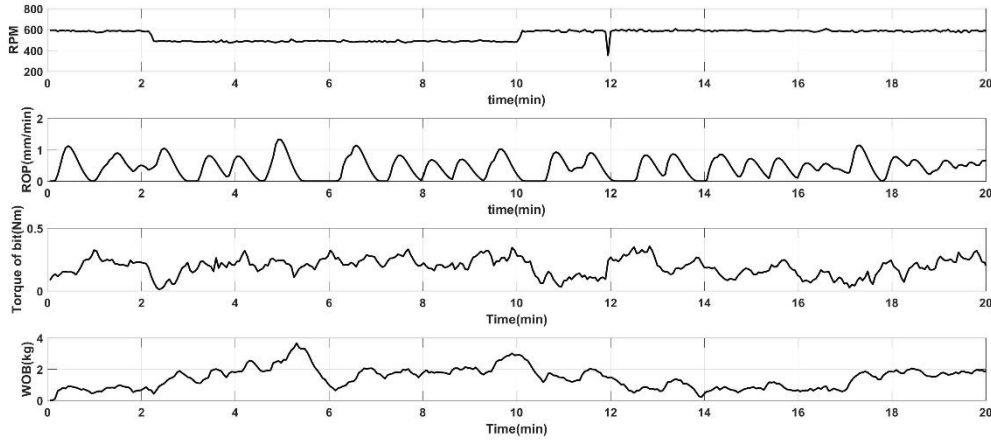


Fig. 5.11: Filtered drilling data for tiles

Above, the torque is converted to bit torque and the z forces are converted to WOB calculations by subtracting from the free weight.

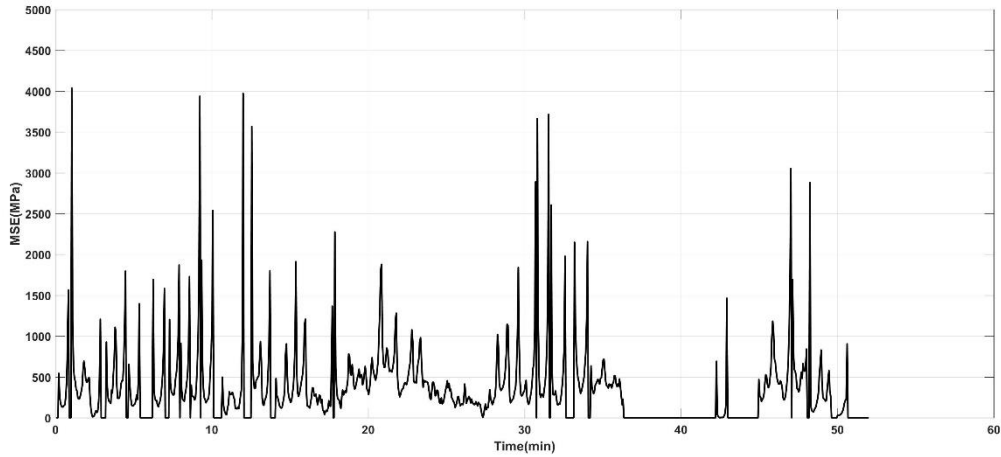


Fig. 5. 12: *Unfiltered MSE data for drilling through tiles*

As shown above, the MSE data has significant noise with large spikes. Thus, an aggressive low pass filter is applied to remove this.

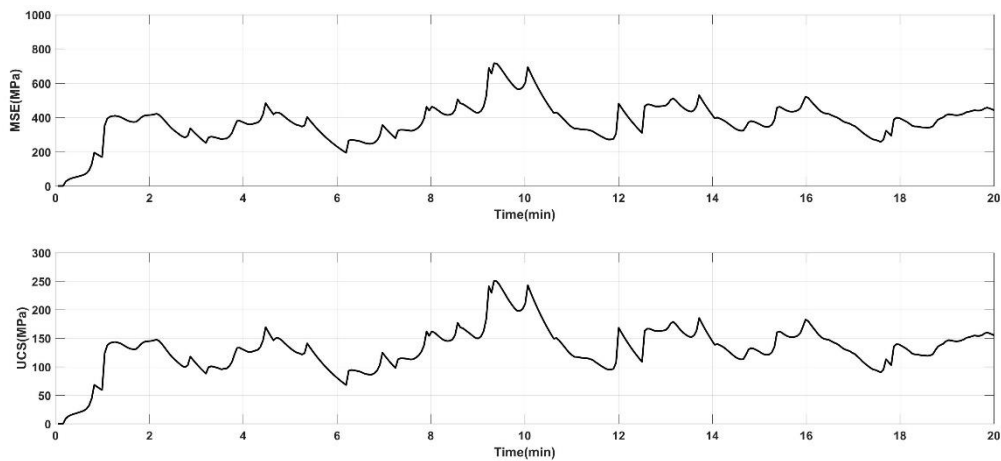


Fig. 5.13: *Filtered MSE data for drilling through tiles*

Above, the UCS is much higher than the cement samples, in the range of 100 – 250 MPa. This corresponds to a classification from Table 3.1 of strong to very strong. This makes sense as the materials used in this rock sample were hardened marble and limestone, which have much higher respective hardness ratings on the Mohr’s hardness scale. This implies that with the implementation of this to real time, that the strength of the drilled rock can be approximated and differentiated from other materials. More importantly, this can give an indication that a new formation has been encountered, and that the drilling parameters for an optimal ROP are no longer valid and a re-sweep of the founders point needs to take place.

Conclusions

Two simplified models were introduced in order to describe the drill-string and BHA in order to be used in the ROP models proposed in this paper.

Filtering is essential for proper drilling coordination and sometimes aggressive filtering techniques are needed. Further work could be done attempting to integrate a Kalman filter or sensor fusion.

Certain deteriorating drilling conditions can be identified and mitigated if proper detection occurs. This is dependent on proper data acquisition and proper filtering.

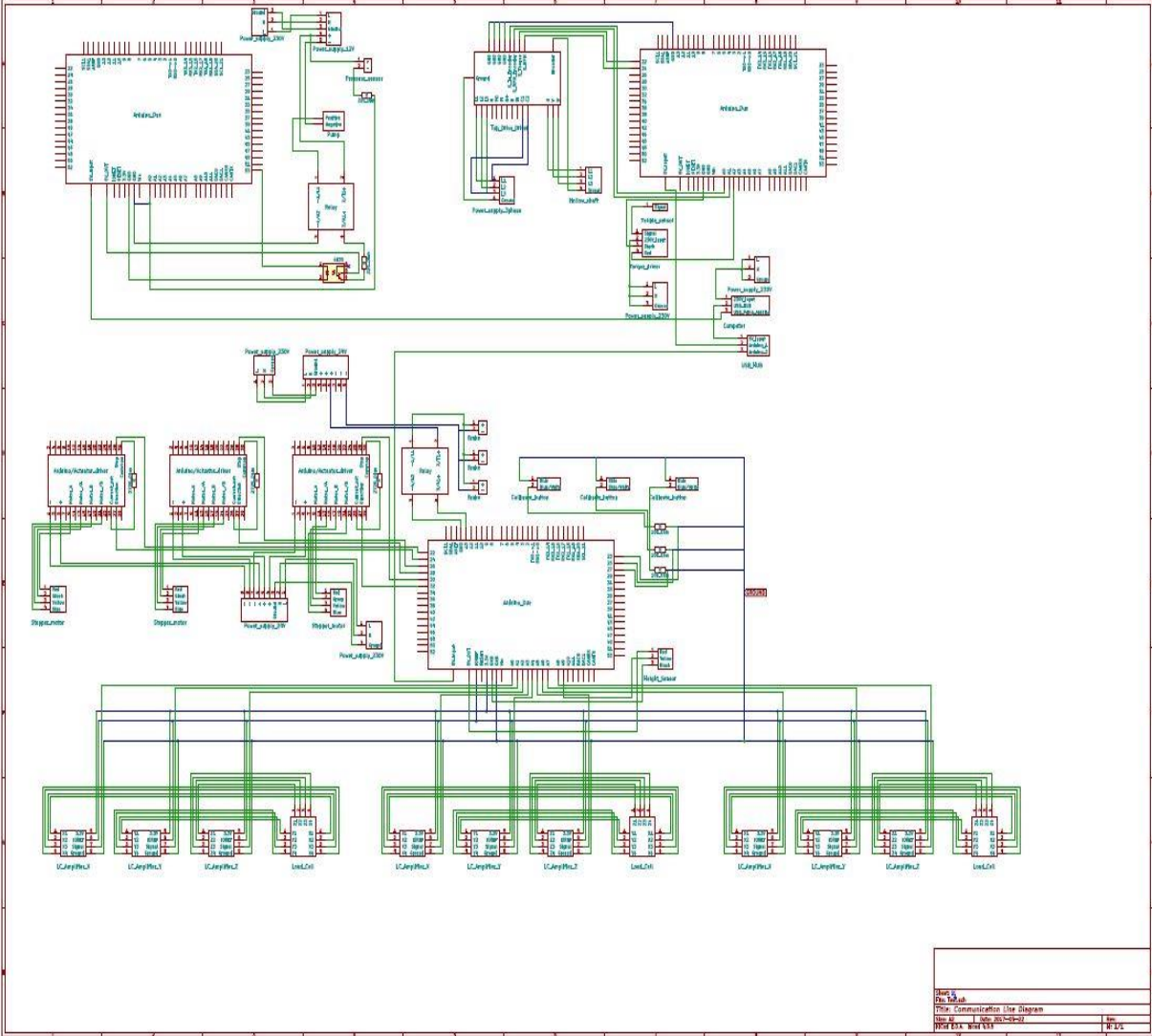
UCS calculations can be used to detect rock strengths and thus new formations if the rock strength change is great enough with the use of filtering. However, a way needs to be found to calculate this in real time in order to autonomously react in order to sweep for new optimal parameters.

References

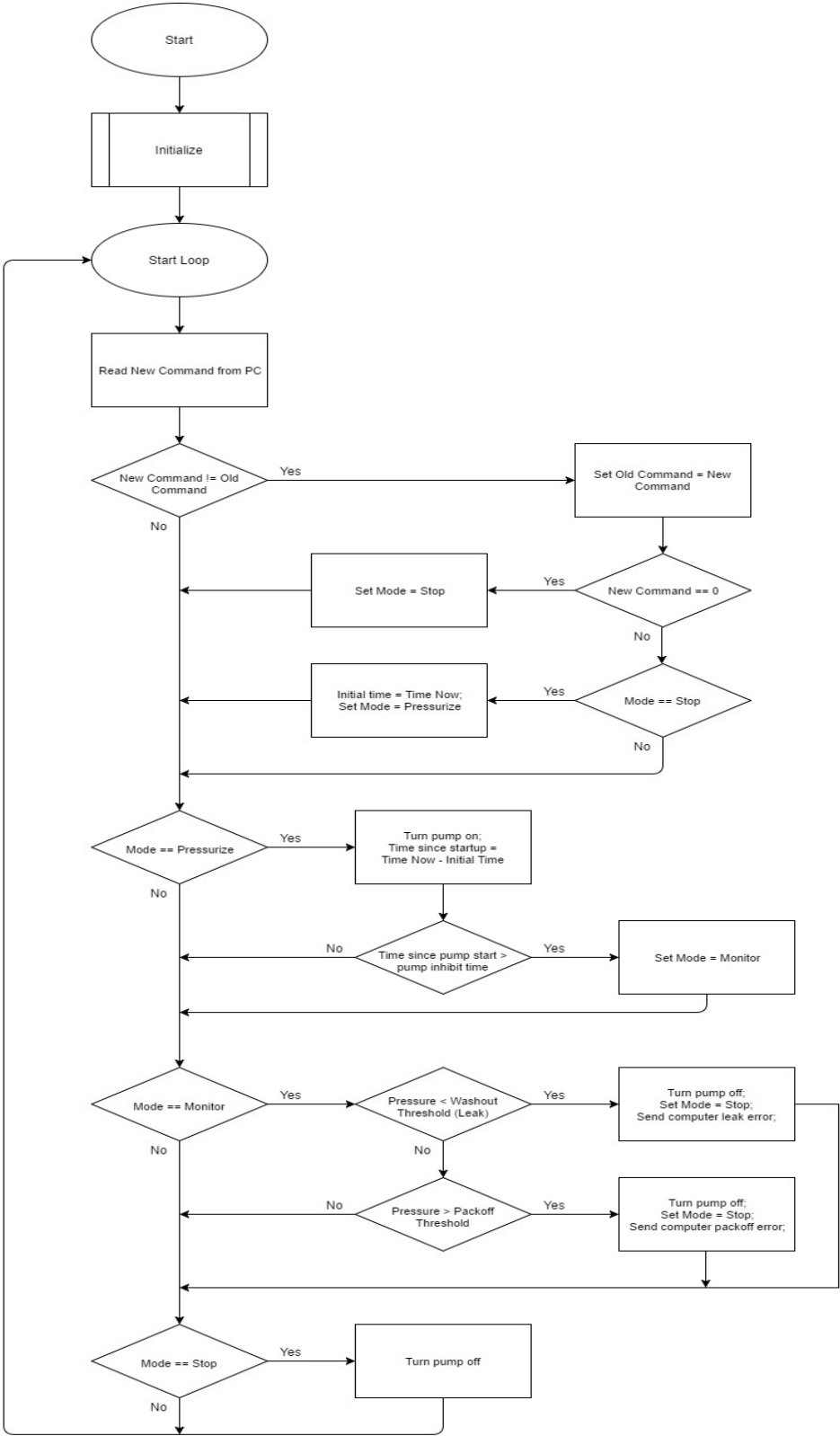
- [1] Omar Salem Alani. Management of drilling incidents while drilling heterogenous formation rocks, June 2016.
- [2] The Drilling Systems Automation Technical Section, “Drillbotics,” 2015. [Online]. Available: www.Drillbotics.com.
- [3] Todd Robert Hamrick. Optimization of Operating Parameters for Minimum Mechanical Specific Energy in Drilling. Master's thesis, West Virginia University, 2011.
- [4] Eric Cayeux and Hans Joakim Skadsem. Modelling of the Dynamic Behavior of the Power Transmission of an Automatic Small Scale Drilling Rig, June 2017.
- [5] Morten Krøtøy Johannessen and Torgeir Myrvold. Stick-Slip Prevention of Drill Strings Using Nonlinear Model Reduction and Nonlinear Model Predictive Control, May 2010.
- [6] Internal Lecture Notes Provided by Dan Sui.
- [7] Dan Sui. Real-time Drilling Rate Optimization for Hole Cleaning Efficiency during Drilling Operations.
- [8] Eric Cayeux et al. Challenges in the Automation of Lab-Scale Drilling Rig vs Full Scale Rig. Society of petroleum engineers. April 2017.
- [9] Olaleke Anthony Akisanmi. Automatic Management of Rate of Penetration in Heterogeneous Formation Rocks, 2016.
- [10] Alexander Trulsen and Erik Andreas Løken. Construction, Design and Optimization of an Autonomous Laboratory-Scale Drilling Rig, May 2017.
- [11] Attewell, P., Farmer, I., 1976, Principles of engineering geology.
- [12] http://www.dfe.com/resources/faq_openloopvsclosedloop.html
- [13] https://en.wikipedia.org/wiki/PID_controller

Appendix

Appendix A – Electrical/Control Lines



Appendix B - Circulation Microcontroller Decision Tree



Appendix C - Hoisting Interrupt Service Routine Responsible for Moving Actuators

```
void stepInterrupt() {
    if (!_isSetup) return;
    int pushButton = digitalRead(_endStopperPin);
    if (pushButton == HIGH) {
        _endStopperMeasurements++;
        if (_endStopperMeasurements > 5) {
            _trustedEndStopper = true;
            _position = 0.0;
        }
    }
    else {
        _endStopperMeasurements = 0;
        _trustedEndStopper = false;
    }

    if ((_StepCounter <= 0)
        || ((_trustedEndStopper == true) && (_direction == UP))
        || (_brakeStatus == CLOSED))
    {
        _StepCounter = 0;
        // don't do anything
    }
    else {
        digitalWrite(_pulsePin, _step_wire_on = !_step_wire_on);
        _StepCounter--;
        if (_direction == UP)
        {
            //raising
            _position = _position - (0.5 / STEPS_PER_DISTANCE); //dividing by
2 because everytime we enter the interrupt it only executes half a pulse
        }
        else if (_direction == DOWN)
        {
            //lowering
            _position = _position + (0.5 / STEPS_PER_DISTANCE); //dividing by
2 because everytime we enter the interrupt it only executes half a pulse
        }
    }
}
}
```